Atmospheric fate of a series of saturated alcohols: kinetic and mechanistic study

Inmaculada Colmenar[1,2], Pilar Martin[1,2], Beatriz Cabañas[1,2], Sagrario Salgado[1,2], Araceli Tapia[1,2], Inmaculada Aranda[1,2]

[1]Universidad de Castilla La Mancha, Departamento de Química Física, Facultad de Ciencias y Tecnologías Químicas, Avda. Camilo José Cela S/N, 13071 Ciudad Real, Spain

[2]Universidad de Castilla La Mancha, Instituto de Combustión y Contaminación Atmosférica (ICCA), Camino Moledores S/N, 13071 Ciudad Real, Spain

Correspondence to: Pilar Martín (mariapilar.martin@uclm.es)

Keywords. Saturated alcohols, additives, biofuel, atmosphere, reactivity.

Abstract. The atmospheric fate of a series of saturated alcohols (SAs) has been evaluated through the kinetic and reaction product studies with the main atmospheric oxidants. These SAs are alcohols that could be used as fuel additives. Rate coefficients (in cm^3 molecule^{-1} s^{-1} unit) measured at ~298K and atmospheric pressure (720 ± 20 Torr) were as follows: k_1 (E-4-methyl-cyclohexanol + Cl) = $(3.70 \pm 0.16) \times 10^{-10}$, k_2 (E-4-methyl-cyclohexanol + OH) = $(1.87 \pm 0.14) \times 10^{-11}$, k_3 (E-4-methyl-cyclohexanol + NO$_3$) = $(2.69 \pm 0.37) \times 10^{-15}$, k_4 (3,3-dimethyl-1-butanol + Cl) = $(2.69 \pm 0.16) \times 10^{-10}$, k_5 (3,3-dimethyl-1-butanol + OH) = $(5.33 \pm 0.16) \times 10^{-12}$, k_6 (3,3-dimethyl-2-butanol + Cl) = $(1.21 \pm 0.07) \times 10^{-10}$ and k_7 (3,3-dimethyl-2-butanol + OH) = $(10.50 \pm 0.25) \times 10^{-12}$. The main products detected in the reaction of SAs with Cl atoms (absence/presence of NO$_x$), OH and NO$_3$ radicals were: E-4-methylcyclohexanone for the reactions of E-4-methyl-cyclohexanol, 3,3-dimethylbutanal for the reactions of 3,3-dimethyl-1-butanol and 3,3-dimethyl-2-butanone for the reactions of 3,3-dimethyl-2-butanol. Other products such as formaldehyde, 2,2-dimethylpropanal and acetone have also been identified in the reactions of Cl atoms and OH radicals with 3,3-dimethyl-1-butanol and 3,3-dimethyl-2-butanol. In addition, the molar yields of the reaction products were estimated. The products detected, indicate a hydrogen atom abstraction mechanism at different sites on the carbon chain of alcohol in the case of Cl reactions and a predominant site in the case of OH and NO$_3$ reactions, confirming the predictions of Structure Activity Relationship (SAR) methods. Tropospheric lifetimes (τ) of these SAs have been calculated using the experimental rate coefficients. Lifetimes are in the range of 0.6-2 days for OH reactions, 7-13 days for NO$_3$ radical reactions and 1-3 months for Cl atoms. In coastal areas the lifetime due to the reaction with Cl decreases to hours. The calculated global tropospheric lifetimes, and the polyfunctional compounds detected as reaction products in this work, imply that the SAs could contribute to the formation of ozone and nitrated compounds at local, regional and even to global scale. Therefore, the use of saturated alcohols as additives in diesel-blends should be considered with caution.

1. Introduction

A multitude of scientific studies on combustion emissions confirm that fossil fuels, especially diesel fuel, are the substances mainly responsible for air pollution. The loss of air quality and its consequences for health as well as for global warming are some of the most important problems caused by air pollution (www.iea.org). These consequences have led governments to set restrictive limits on the presence of certain pollutants in the atmosphere, such as the case of particulate matter (PM) (EURO 6) and to develop biofuels (Sikarwara et al., 2017) as alternatives to conventional ones. Biodiesel is obtained from the transesterification of oils animal or vegetable origin. Also, the fermentation of vegetal biomass gives methanol and or ethanol (bioethanol). These lower alcohols have been used as fuels and show advantages such as the reduction in smoke, due to the presence of the OH group that increases the oxygen content during the combustion process (Ren et al., 2008; Lapuerta et al., 2010; Sarathy et al., 2014; Sikarwara et al., 2017). However, several studies have shown certain complications in the use of lower alcohols due to their low cetane number, the high latent heat of vaporization and high resistance to auto-ignition (Karabektas and Hosoz, 2009). In order to avoid or to minimize these limitations, alcohol–diesel blends and alcohol–diesel emulsions have been used in diesel engines (Ozsezen et al., 2011). Another alternative is the use of longer-chain alcohols (propanol, n-butanol, isobutanol and n-pentanol) with superior fuel properties than lower alcohols when mixed with diesel fuel (Cheung, et al., 2014; Kumar and Saravanan, 2016; Li et al., 2017).

Alcohols are present in the atmosphere from a wide variety of anthropogenic and biogenic sources (Calvert et al., 2011). Methanol, ethanol and isopropanol are some of the main alcohols detected in urban areas such as Osaka and Sao Paulo cities (Nguyen et al., 2001) with concentrations of 5.8−8.2 ppbv and 34.1−176.3 ppbv respectively. Other alcohols, such as E-4-methylcyclohexanol, have been identified in the exhaust gas emissions resulting from burning fuel blends containing 7% v/v (B7) and 20% v/v (B20) of soy bean/palm biodiesel (84%/16%) (Lopes et al., 2014). 3,3-dimethyl-1-butanol is a glass-forming material used as a chemical intermediate in organic syntheses (www.capotchem.com). 3,3-dimethyl-2-butanol is a potential precursor for prohibited chemical weapons such as soman, a nerve agent (Murty et al., 2010). It is also used in conversion of ribose-and glucose- binding proteins into receptors for pinacolyl methyl phosphonic acid (Allert et al. 2004). The use of long-chain alcohols as biofuels could present an additional important source of these alcohols in the atmosphere. Therefore, prior to use, it is necessary to study the reactivity of long-chain alcohols in atmospheric conditions in order to establish and to evaluate their atmospheric impact.

In the case of small alcohols, the knowledge of their reactivity is well established and indicates that the main degradation process of saturated alcohols in the atmosphere is the reaction with hydroxyl radicals (OH) during the daytime (Grosjean et al., 1997; Atkinson and Arey, 2003; Atkinson et al., 2006; Calvert et al., 2011; Caravan et al., 2015; Mellouki et al, 2015). Kinetics with chlorine atoms (Cl) are expected to be high, therefore reactions with Cl could also be an important degradation route, especially in coastal areas where concentration peaks of Cl atoms can be found. Reactions with ozone molecular (O_3) ($k \leq 10^{-20}$ cm^3 molecule^{-1} s^{-1}) and nitrate radical (NO_3) ($\sim 10^{-15}$ cm^3 molecule^{-1} s^{-1}) are too low to make a significant contribution to their degradation. However, the determination of the rate coefficients and the reaction products of alcohols with the nitrate radical are also necessary to understand better the general reactivity of alcohols in the atmosphere, since the reactions with this radical are a source of OH during the night-time (Finlayson-Pitts and Pitts, 2000).
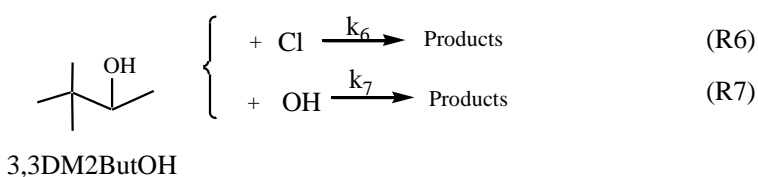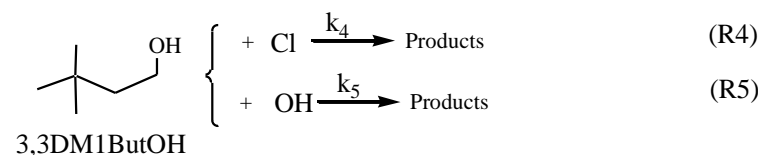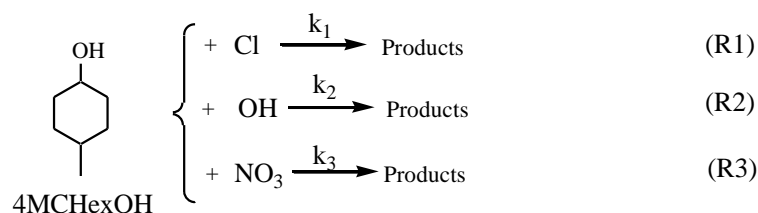
1 Although in last years some studies into the reactivity of higher alcohols have been made (Ballesteros et al., 2007;

2 Hurley et al., 2009; Andersen et al., 2010; Calvert et al., 2011; Moreno et al., 2012, 2014, Mellouki et al., 2015)

3 the kinetic and mechanistic database is still scarce. In the case of 3,3-dimethyl-1-butanol and 3,3-dimethyl-2-

4 butanol (derivates of 1-butanol and 2-butanol) there is a lack of information with respect to the diurnal reactivity

5 (Moreno et al., 2014; Mellouki et al., 2015). Regarding cyclic alcohols, only data concerning the reactivity of

6 chlorine atoms and OH radicals with cyclohexanol (Bradley et al., 2001; Ceacero-Vega et al., 2012) and OH with

7 cyclopentanol (Wallington et al., 1988) have been reported.

8 Therefore, in the present work studies into the kinetics and the products of gas-phase reactions of some SAs, such

9 as E-4-methylcyclohexanol (4MCHexOH), 3,3-dimethyl-1-butanol (3,3DM1ButOH) and 3,3-dimethyl-2-butanol

10 (3,3DM2ButOH) with Cl atoms and OH and NO_3 radicals have been carried out. These SAs have been chosen for

11 their potential use as biofuels and because their reactivity has not yet been evaluated. So, our work will permit to

12 complete the kinetic and mechanism database, to improve our knowledge of the atmospheric chemistry of higher

13 alcohols and to assess their environmental chemical impact in the case of their future use as biofuels.

14 **2. Experimental Section**

15 **2.1 Kinetic experiments**

16 The reactions of a series of SAs with the main atmospheric oxidants have been studied:

$$+ \; Cl \; \xrightarrow{k_1} \; Products \qquad (R1)$$

$$+ \; OH \; \xrightarrow{k_2} \; Products \qquad (R2)$$

$$+ \; NO_3 \; \xrightarrow{k_3} \; Products \qquad (R3)$$

4MCHexOH

$$+ \; Cl \; \xrightarrow{k_4} \; Products \qquad (R4)$$

$$+ \; OH \; \xrightarrow{k_5} \; Products \qquad (R5)$$

3,3DM1ButOH

$$+ \; Cl \; \xrightarrow{k_6} \; Products \qquad (R6)$$

$$+ \; OH \; \xrightarrow{k_7} \; Products \qquad (R7)$$

3,3DM2ButOH

17

18

19 Rate coefficients were determined using a relative rate method. This method relies on the assumption that the

20 organic compound (SA) and the reference compound (R), are removed solely by their reactions with the oxidants

21 (Ox: OH and NO_3 radicals and Cl atoms):

22 $\qquad\qquad$ Ox + SA → Products (k_{SA}) $\qquad\qquad\qquad$ (R8)

23 $\qquad\qquad$ Ox + R → Products (k_R) $\qquad\qquad\qquad$ (R9)

24 where k_{SA} and k_R are the rate coefficients of the SA and the reference compound, respectively.

25 On the assumption that the SA and the reference compound are only consumed by reaction with the oxidants, the

26 kinetic treatment for the reactions expressed by R8 and R9 gives the following relationship;

$$ln\left(\frac{[SA]_0}{[SA]_t}\right) = \frac{k_{SA}}{k_R} ln\left(\frac{[R]_0}{[R]_t}\right) \qquad (1)$$

where $[SA]_0$, $[R]_0$, $[SA]_t$, and $[R]_t$ are the initial concentrations and those at time t for the SA and the reference compound, respectively. Two reference compounds were used with each oxidant to ensure that the reference compound had no influence on overall rate coefficient.

According to Eq (1), a plot of $ln([SA]_0/[SA]_t)$ versus $ln([R]_0/[R]_t)$ should be a straight line that passes through the origin. The slope of this plot gives the ratio of rate coefficients k_{SA}/k_R. Therefore, the value of k_{SA} can be obtained if the rate coefficient k_R of the reference compound is known.

The experimental systems have been described in previous works (Tapia et al., 2011; Martin et al., 2013) and only a brief description is given here. Kinetic measurements were performed at room temperature (~298 K) and atmospheric pressure (720 ± 20 Torr) by employing two separate experimental set-ups: 1) A 50 L Pyrex® glass reactor was coupled to an Fourier Transform Infrared spectrometer as a detection technique ("on-line" analysis). Inside of the Pyrex® glass reactor there is a multi-reflection system with three mirrors that allows an infrared radiation path of 2.8−200 m. This reactor is known as white cell (Saturn Series Multi-Pass cell). The FTIR spectrometer (Thermo Nicolet 6700) was equipped with a KBr beam splitter and liquid nitrogen-cooled MCT. Typically, for each spectrum, 60 interferograms were co-added over 98 s and approximately 30−40 spectra were recorded per experiment with a spectral resolution of 1 cm^{-1}. 2) A Teflon ® gas bag reactor of 500 L with solid phase micro extraction (SPME) for sampling and gas chromatography with a time of flight mass spectrometer (SPME/GC-TOFMS) (AccuTOF GCv, Jeol) ("off-line" analysis). Samples were collected by exposing a 50/30 mm DVB/CAR/PDMS SPME (SUPELCO) for 5 min during the reaction and then thermally desorbed for 15 min at 250 ℃ in the heated GC injection port. A capillary column (30 m × 0.3 mm id × 1.0 mm film thickness, Tracsil TRB-1701, Teknokroma) was used to separate the compounds. The chromatographic conditions used for the analysis were as follows: injector, 250 ℃; interface, 250 ℃; initial oven temperature, 40 ℃ for 4 min; ramp, 30 ℃ min^{-1} to 120 ℃, held for 6 min; second ramp, 30 ℃ min^{-1} to 200 ℃, held for 3 min.

In each independent experiment, the reactants were injected into the reactors from a vacuum line by dragging with a stream of carrier gas used in the reaction. Both reactors were inside a metallic housing in the walls of which there is a rack of actinic lamps (Philips, TL-40 W, Actinic BL, λ_{max} = 360 nm). A scheme of the experimental systems is shown in Fig. S1, Supplementary Material.

The kinetic experiments for the Cl and OH reactions were performed in the 50 L Pyrex® glass reactor coupled to an FTIR spectrometer. A spectral subtraction procedure was used to derive the concentrations of reactant and reference compounds at time t = 0 and time t. The reaction of NO_3 with 4MCHexOH was studied using a 500 L Teflon® reactor in order to minimize the wall deposition and dilution effects of consecutive additions of N_2O_5. Chlorine atoms and OH radicals were obtained by photolysis of Cl_2 in N_2 and methyl nitrite, CH_3ONO, in the presence of NO in air. Methyl nitrite was synthesized in the laboratory as described elsewhere (Taylor et al., 1980). Nitrate radicals were generated in situ in the dark by the thermal decomposition of N_2O_5 (Atkinson et al., 1984, 1988). N_2O_5 was obtained mixing O_3 with an excess of NO_2 (Scott and Davidson, 1958). Prior to the kinetic experiments a series of tests in the dark and photolytic conditions were carried out to evaluate secondary reactions, such as wall depositions and photodegradation of all reactants.

1   The range concentrations of reactants employed were as follows: 2−16 ppm of 4MCHexOH, 3−9 ppm of

2   3,3DM1ButOH and 3,3DM2ButOH, 9−30 ppm of Cl_2, 4−13 ppm of 1-butene and 2-methylpropene, 7−14 ppm of

3   propene and cyclohexene, 5−7 ppm of isopropanol, 3−5 ppm of 2-methyl-2-butanol, 26−55 ppm of CH_3ONO,

4   20−60 ppm of NO, 3−4 ppm of 2-ethyl-1-hexanol, 4−5 ppm of 1-butanol. For reactions of 4MCHexOH with

5   nitrate radicals 2−5 additions of N_2O_5 with concentrations between 8−36 ppm were made per experiment.

6   **2.2 Product experiments**

7   The product study was carried out at room temperature (~ 298 K) and at a pressure of 720 ± 20 Torr of synthetic

8   air employing the two experimental set-ups previously described. In some experiments carried out in the 50 L

9   Pyrex® reactor, simultaneous identification of products was performed using both detection techniques. For that,

10 one sample of reaction mixture was taken from this reactor using the SPME and subsequently analyzed with GC-

11 TOFMS. In addition, independent experiments using SPME/GC-TOFMS in a 150 L Teflon® reactor were

12 developed. Product analyses were carried out using the same procedure as for the kinetic experiments, without the

13 reference compound, and employing synthetic air as bath gas. On this occasion the heating of the oven was changed

14 slightly in order to get a better separation and to detect the products generated. The temperature ramps of the oven

15 employed in the chromatograph were: 40 ℃ for 4 min; ramp, 25 ℃ $min^{−1}$ to 120 ℃, held for 10 min; second ramp,

16 25 ℃ $min^{−1}$ to 200 ℃, held for 4 min.

17 The qualitative analysis in the FTIR experiments was carried out using the FTIR library that provided the FTIR

18 spectrophotometer   (Aldrich   vapor   phase   sample   library,

19 https://www.thermofisher.com/search/browse/results?customGroup=Spectral+Libraries)   and/or   the   FTIR

20 database of Eurochamp (https://data.eurochamp.org/data-access/spectra/).

21 For the SPME/GC-TOFMS experiments, the NIST webbook (https://webbook.nist.gov/chemistry/) and the mass

22 spectra database of the instrument were used to identify the products. Calibrated FTIR spectra and SPME/GC-

23 TOFMS chromatograms were used for quantification in those cases where the product was commercially available.

24 The molecular yields of the reaction products were estimated from the slopes of plots of the concentration of

25 product formed versus the amounts of SA (Δ[SA]) consumed. In the cases where an important loss of the reaction

26 product by reaction of the oxidant and/or by photolytic process was observed, the concentration of the product was

27 corrected using the formulism of Tuazon et al. (1986) (See S1, Supplementary Material). Range of concentrations

28 of reactants employed were as follows: 2−14 ppm of SA, 8−31 ppm of Cl_2, 12−57 ppm of NO, 19−66 ppm of

29 CH_3ONO and 6−36 ppm of N_2O_5.

30 Chemicals used were as follows: 4MCHexOH (97%, Aldrich), 3,3DM1ButOH and 3,3DM2ButOH (98%,

31 Aldrich); 1-butene, propene, 2-methyl-2-butanol, isopropanol, 2-methylpropene, 4-methylcyclohexanone and

32 cyclohexene (≥99%, Aldrich), 2-ethyl-1-hexanol (≥ 99%, Fluka), 1-butanol (99.8%, Aldrich), 3,3-dimethylbutanal

33 (95%, Aldrich) and 3,3-dimethyl-2-butanone (98%, Aldrich), NO (99%, Praxair), Cl_2 (> 99.8%, Praxair), synthetic

34 air (Praxair Ultrahigh purity 99.999%) and N_2 (99.999%, Praxair). For N_2O_5 synthesis, N_2O_4 was used (>99.5%)

35 from Fluka, P_2O_5 (98%, such as desiccant) from Fluka and O_3 was synthesized by a generator model TRCE-5000,

36 5 g_{O3} h^{-1} OZOGAS.

37 **3. Results and Discussion**

3.1 Kinetic study

Preliminary test experiments indicated that dark heterogeneous reactions and photolytic losses of SAs and reference compounds could be considered negligible in our experimental conditions ($k \approx 10^{-6}$ s^{-1}). The kinetic study was carried out at room temperature ($\sim$298 K) and at 720 ± 20 Torr of N$_2$ gas for Cl atoms reactions and synthetic air for OH radical reactions. Nitrate radical experiments were performed using N$_2$ gas in a 500 L Teflon reactor and employing the SPME/GC-TOFMS system. A number of injections of the unreacted mixture were carried out in order to determine the associated precision of the sampling method to be used in the error analysis (Brauers and Finlayson-Pitts, 1997). The standard deviations (σ) were as follows: 3.7% for 4MCHexOH, 1.7% for 1-butanol and 3.5% for 2-ethyl-1-hexanol.

Figure 1 shows examples of the kinetic data plotted according to Eq (1) for the reactions of SAs with different atmospheric oxidants. A good correlation was obtained with an intercept close to zero, which indicated the absence of secondary reactions. From the slopes of the plots (k_{SA}/k_R) and knowing the values of the rate coefficients for the reference compounds employed (k_R), the value of the absolute rate coefficient for each saturated alcohol (k_{SA}) was determined. Rate coefficients of reactions of reference compounds with Cl atoms reactions (in 10^{-10} cm^3 molecule^{-1} s^{-1} units) were: 2-methylpropene (3.40 ± 0.28), 1-butene (3.38 ± 0.48), (Ezzel et al., 2002) and propene (2.23 ± 0.31) (Ceacero-Vega et al., 2009); with OH radicals (in 10^{-11} cm^3 molecule^{-1} s^{-1} units): propene (2.66 ± 0.40) (Atkinson and Aschman, 1989), cyclohexene (6.77 ± 1.69) (Atkinson and Arey, 2003), isopropanol (0.51 ± 0.008) (IUPAC www.iupac-kinetic.ch.cam.ac.uk) and 2-methyl-2-butanol (0.36 ± 0.06) (Jiménez et al., 2005) and with NO$_3$ radicals (in 10^{-15} cm^3 molecule^{-1} s^{-1} units): 1-butanol (3.14 ± 0.97) and 2-ethyl-1-hexanol (2.93 ± 0.92) (Gallego-Iniesta et al., 2010).

The ratios of the rate coefficients, k_{SA}/k_R, the absolute rate coefficients and the weighted averages are shown in Table 1. The error of k_{SA}/k_R was given by two times the statistical deviation calculated from the least squares fit of the plot of Eq. (1). The uncertainties for rate coefficients of SA (σ_{kSA}) were calculated from the uncertainty of slope of plots (σ_{slope}) and the uncertainty of the reference (σ_{kR}) by using the propagation of uncertainties. The average value of the rate coefficients obtained with different reference compounds and their associated errors were obtained by weighted average (See footnote, Table 1). The rate coefficients obtained in this work are the first kinetic data reported for these SAs therefore, the results obtained cannot be compared with literature values.

It is well established that the gas-phase reaction mechanism of saturated organic compounds (alkanes, alcohols, ethers, etc.) with atmospheric oxidants (Cl atoms, OH and NO$_3$ radicals) are initiated via hydrogen atom abstraction from the organic compound to form a stable molecule and an alkyl radical (Finlayson-Pitts and Pitts, 2000; Atkinson and Arey, 2003; Calvert et al., 2011; Ziemann and Atkinson, 2012). The presence of the OH group in saturated alcohols implies two types of hydrogens that can be abstracted: hydrogen bonded to a carbon (C−H) of the main chain or of an alkyl substituent and hydrogen bonded to oxygen of OH group. Two literature reviews of the reactivity of saturated alcohols (Calvert et al., 2011; Mellouki et al., 2015) conclude that: 1 − The reactions of aliphatic alcohols with atmospheric oxidants proceed mainly by H atom abstraction from various C−H groups in the alkyl chain, abstraction of H atom from the O−H group being negligible; 2 − Rate coefficients for the reactions of Cl, OH and NO$_3$ are higher for alcohols than those of the corresponding alkanes due to the activating effect of the OH group. This effect is extended over about four carbon atoms (Nelson et al., 1990); and 3 − The attack

1 percentage of a radical to the different sites of the alcohol (α, β, γ and δ) depends on the oxidant, the structure of

2 saturated alcohol, the type and numbers of substituents, and temperature (Moreno et al., 2012, 2014; McGillen et

3 al., 2013, 2016).

4 In order to verify these remarks, the reactivity of the SAs studied in this work were analyzed and discussed by

5 comparing the rate coefficients of the SAs obtained with different oxidants; comparing the rate coefficients of the

6 SAs and the rate coefficients of their homologous alkanes available in literature, and comparing the rate

7 coefficients obtained in the reaction of the same oxidant but with different alcohols. The data used in the

8 comparison are summarized in Table S1 in Supplementary Material.

9 From the analysis of all data shown in Table S1, it can be observed that:

10 a) The trend in the reactivity of SAs in relation to the different oxidants is the same that observed for other saturated

11 alcohols: k_{Cl} ($k \approx 10^{-10}$) > k_{OH} ($k \approx 10^{-11}$) >> k_{NO3} ($k \approx 10^{-15}$), (k in cm^3 molecule^{-1} s^{-1} units). This behavior could

12 be explained by considering the geometry and electronic density of each oxidant, together with kinetic collision

13 theory. As the Cl atom has spherical electronic density distribution, any collision orientation is suitable, in addition,

14 the Cl atoms present low steric hindrance. So the Cl reaction is comparatively less selective and faster, with values

15 for the rate coefficient, k, in the collision limit. However, the OH radical presents an asymmetric electron density

16 located mostly over its oxygen atom. Therefore, for the OH reaction the oxygen of the OH radical must be

17 specifically oriented toward the hydrogen of the SA that will be abstracted. The electronic density of nitrate radical

18 is distributed around the three oxygens, which implies several appropriate orientations, but since the nitrate radical

19 has a non-linear structure, the steric hindrance is much greater than for the OH radical, which reduces the reactivity

20 of NO_3 in relation to that of OH.

21 b) The rate coefficient for the reaction of 4MCHexOH with Cl atoms is similar to the rate coefficient of its

22 homologous alkane (E-1,4-dimethylcyclohexane): $k_{4MCHexOH+Cl}$ = 37.0×10^{-11} $\approx$ $k_{E\text{-}1,4\text{-}dimethylcyclohexane+Cl}$

23 = 36.3×10^{-11}. In the case of the reaction with OH radical, the rate coefficient of 4MCHexOH is 1.5 times higher

24 than with E-1,4-dimethylcyclohexane: $k_{4MCHexOH+OH}$ = 18.7×10^{-12} > $k_{E\text{-}1,4\text{-}dimethylcyclohexane+OH}$ = 12.1×10^{-12} (Table

25 S1). These results show that the activating effect of the OH group of the SA is less important for the reaction with

26 Cl atoms than with the OH radical, behavior that agrees with that established by the Structure Activity

27 Relationships (SARs) methods (Kwok and Atkinson 1995; Calvert et al. 2011). There are no rate coefficient data

28 for the reactions with NO_3 radical of the alkanes homologous to the SAs studied in this work, and therefore it was

29 not possible to check the effect of OH group in the reaction with NO_3. However, according to the SAR method

30 developed by Kerdouci et al. (2010) for the reactions of alcohols with NO_3, this effect is greater than in the

31 corresponding Cl and OH reactions.

32 c) The activating effect of the chain length in the reactivity of alcohols is also different for the Cl and OH reactions

33 (See Table S1). Furthermore, if the rate coefficients of 3-methyl-1-butanol (3M1ButOH) and 3,3DM1ButOH with

34 Cl and OH are compared, a slight increase in the rate coefficient for Cl reaction can be observed ($k_{3M1BuOH+Cl}$ =

35 25.0×10^{-11}; $k_{3,3DM1ButOH+Cl}$ = 26.9×10^{-11}) together with an important decrease in the rate coefficient for the OH

36 reactions ($k_{3M1BuOH+OH}$ = 14×10^{-12}; $k_{3,3DM1ButOH+OH}$ = 5.33×10^{-12}). This behavior could be explained by the

37 different order of reactivity of the two oxidants. So, Cl atom, more reactive (k in the order of 10^{-10} cm^3 molecule^{-1}

38 s^{-1}) but less selective than OH, an increase in the chain length or in the number of methyl groups in the SA implies

39 more hydrogens available to be abstracted and therefore an increase in the rate coefficient. However, for OH

radicals, less reactive (k in the order of $10^{-11}-10^{-12}$ cm^3 molecule^{-1}s^{-1}) and more selective than Cl, the attack for H-abstraction will be carried out at a specific position in the SA, so an increase in the chain length of the alcohol does not have a significant effect on the reactivity; the presence of a second methyl group even disfavors the reaction, probably due to steric hindrance near the attack position.

In addition, as can be seen in Table S1, the position of the OH group of SA has a different effect on the reactivity depending on the oxidant. In the case of the Cl atom reactions, the rate coefficients for primary alcohols (1-propanol, 1-butanol, 1-pentanol, 3-methyl-1-butanol and 3,3-dimethyl-1-butanol) are higher than the those of secondary alcohols (2-propanol, 2-butanol, 2-pentanol, 3-methyl-2-butanol and 3,3-dimethyl-2-butanol) contrary to the OH and NO$_3$ radical reactions. This indicates that in the reaction of Cl atoms the formation of the most stable radical seems to have less importance in the reactivity than the number of hydrogens in the α−position available to be abstracted.

All these observations could imply a different mechanism for the hydrogen abstraction process for Cl atoms versus the OH radical. Nelson et al. (1990) and Smith and Ravishankara (2002) indicate the possible formation of an intermediate adduct between the OH radical and the oxygen of the OH group that will imply a specific orientation. Theoretical studies found in the literature show this different hydrogen abstraction process in the reaction of saturated alcohols with Cl atoms (Garzon et al., 2006) and OH radical (Moc and Simmie, 2010). There are not enough rate coefficient data for the reaction of SAs with NO$_3$ radicals to establish conclusions about the mechanism. Different mechanisms in the hydrogen atom abstraction process for each oxidant will imply different product distributions and molecular yields, as will be shown in the section on product and mechanism study.

3.1.1 Estimation of rate coefficients

In order to estimate the rate coefficients of the reactions of organic compounds with the atmospheric oxidants, a multitude of methods have been proposed (Vereecken et al., 2018). The most popular and widely used is the SAR method developed initially by Kwok and Atkinson (1995) to estimate the rate coefficients at room temperature for gas-phase reactions with the OH radical. This method has been updated for OH reactions (Jenkin et al., 2018) and extended to reaction with NO$_3$ (Kerdouci et al., 2010, 2014) and Cl (Calvert et al., 2011; Poutsma 2013). The EPA (United States Environmental Protection Agency) has developed the EPI Suite™-Estimation Program Interface that allows estimation of the rate coefficients for the reactions of the OH radical with organic compounds using the AOPWIN v1.92 program.

In our work the rate coefficients of SAs with the three oxidants have been estimated using the SARs method (See S2, Supplementary Material). The results are shown in Table 2. The estimated values of rate coefficients agree with experimental data, with k_{exp}/k_{SAR} ratios between 0.9 and 1.28, except for the case of 3,3DM1ButOH and NO$_3$ radical, which showed a k_{exp}/k_{SAR} ratio of 3.24. In general, the SARs method when applied to alcohols predicts better rate coefficients for the Cl atom and the OH radical than for the NO$_3$ radical, especially for primary alcohols. It is important to note that the kinetic database for the NO$_3$ reactions is more limited than for Cl and OH reactions, so the estimated rate coefficient for NO$_3$ radical should be treated with caution (Kerdouci et al. 2010, 2014; Calver et al., 2011).

It is known that organic compounds that react in the same way with different atmospheric oxidants present a correlation between their rate coefficients. In this sense, over the years, different correlations have been proposed

1   to allow estimation of the unknown rate coefficient when the other is known (Wayne, 1991, 2000; Atkinson, 1994;

2   Calvert et al., 2011; Gallego-Iniesta et al., 2014). The $\log k_{Cl}$–$\log k_{OH}$ and $\log k_{NO3}$–$\log k_{OH}$ correlations have been

3   built for a set of ethers and saturated alcohols by Calvert et al., (2011) obtaining the following relationships:

4    $$\log(k_{Cl}/cm^3\,molecule^{-1}\,s^{-1}) = 0.634 \times \log(k_{OH}/cm^3\,molecule^{-1}\,s^{-1}) - 2.71 \qquad (r^2 = 0.72) \qquad (2)$$

5    $$\log(k_{NO3}/cm^3\,molecule^{-1}\,s^{-1}) = 1.11 \times \log(k_{OH}/cm^3\,molecule^{-1}\,s^{-1}) - 2.42 \qquad (r^2 = 0.66) \qquad (3)$$

6   These equations have been used to estimate the rate coefficients of the reactions of SAs with Cl and NO_3 radical

7   using the experimental rate coefficients measured in this work for OH reactions. The estimated rate coefficients,

8   k_{log}, according to Eqs (2) and (3), and the ratios (k_{exp}/k_{log}), are also shown in Table 2. This estimation method

9   obtains slightly better rate coefficient for 3,3DM1ButOH + NO_3 reaction (k_{exp}/k_{log}. = 1.53) than the SAR method

10   (k_{exp}/k_{SAR} = 3.24). However, for Cl reactions the k_{exp}/k_{log} ratios are in the range of 0.6–1.97, indicating that Eq (2)

11   predicts the rate coefficients worse than SAR method. Again, this could be due to the different reaction mechanism

12   in the H-abstraction process for the Cl and OH reactions. It is important to indicate that in the case of Cl reactions,

13   other effects, such as thermochemistry and the polar effect, must be considered to estimate the rate coefficients for

14   hydrogen abstraction reactions (Poutsma, 2013).

15   **3.2 Product and mechanistic study**

16   A product study of the reaction of 4MCHexOH, 3,3DM1ButOH and 3,3DM2ButOH with chlorine atoms in the

17   absence/presence of NO_x, hydroxyl and nitrate radicals has been performed. IR absorption bands of HCl, CO_2,

18   CO, HNO_3, N_2O, NO_2, HCOOH, HCOH, ClNO, $ClNO_2$ and CH_3NO_3 were observed in the FTIR experiments.

19   Some of these compounds are products from the reactions of the SAs with oxidants. They can also be formed by

20   decomposition of the employed precursors (Cl_2, CH_3ONO and N_2O_5) and in some cases, by heterogeneous

21   reactions of these precursors with the Pyrex glass reactor walls. The formation of O_3 and N_2O_5 have also been

22   observed after long reaction times for the reactions of the SAs with Cl atoms in the presence of NO_x, due to the

23   high concentration of NO_2 in the reaction medium and the presence of radiation. Quantitative analysis was carried

24   out by linear subtraction of a spectrum's absorption bands and the peak areas of GC chromatograms by the use of

25   calibrated spectra and reference chromatograms.

26   The experimental conditions and molecular yields of the main products formed in the reactions of SAs and

27   analyzed by FTIR and SPME/GC-TOFMS are given in Tables 3–6. Molecular yields could be affected by large

28   errors associated with the SPME sampling method and due to the presence of interfering IR absorption bands,

29   mainly associated with precursors of the OH and NO_3 radicals or by nitrated compounds formed.

30   **3.2.1. 4MCHexOH**

31   E-4-methylcyclohexanone was identified in the reactions with Cl (absence/presence of NO_x), OH and NO_3. An

32   example of the product spectra obtained by FTIR is shown in Fig. 2. Formation of E-4-methylcyclohexanone was

33   confirmed by introducing a sample of the commercial product (spectrum (e)). A set of experiments using the SPME

34   as sampling method and the GC-TOFMS as detection technique were also carried out for the reactions of

35   4MCHexOH with Cl atoms and OH and NO_3 radicals. An example of the chromatogram obtained for the reaction

36   of 4MCHexOH with chlorine atoms is shown in Fig. 3. In all the studied reactions, formation of a product peak at

37   10.35 min was observed. The peak (B) shown in Fig. 3 was assigned to E-4-methylcyclohexanone and confirmed

by comparing with the retention time and MS of a commercial sample. In the reactions with Cl atoms (absence/presence of NO_x) and OH radical two additional peaks at 19.80 min (C) and 20.25 min (D) were observed. The time−concentration profiles of 4MCHexOH and E-4-methylcyclohexanone obtained by FTIR analysis for the reaction with Cl atoms in the presence of NO_x are shown in Fig. S2. The concentrations of E-4-methylcyclohexanone, corrected according to Eqs (S1), (S2) and (S3) were plotted versus the amounts of 4MCHexOH consumed in order to obtain the yield of 4-methylcyclohexanone from the slope. An example of the plots obtained is shown in Fig. 4. Molecular yields, Y (%), of E-4-methylcyclohexanone obtained in all experiments are listed in Table 3. Based on the average molecular yield of E-4-methylcyclohexanone, the carbon balance was below to 50% for reactions with Cl and OH radical and ~60% for NO_3.

Residual spectra after subtraction of E-4-methylcyclohexanone show IR absorption bands compatible with the presence of hydroxycarbonyl compounds (~1750, 1720 and 1060 cm^{-1}) and nitrated organic compounds ($RONO_2$ ~1660, 1264 and 862 cm^{-1}, and/or $ROONO_2$ ~1720, 1300 and 760 cm^{-1}) (See residual spectra, Fig. S3 in Supplementary Material). The amount of nitrated compounds was estimated using the average integrated absorption coefficient of 1.2×10^{-17} cm molecule^{-1} of similar compounds corresponding to the IR range 1260−1305 cm^{-1} (Tuazon and Atkinson,1990). The calculated yields of $RONO_2$ were 20% and 60% for Cl (in the presence of NO_x) and NO_3 reactions, respectively. A yield of 10% of nitrated compounds was estimated for the reaction with OH radical. This lower yield could be due to fact that the NO_x, present in the reaction medium reacts faster with the CH_3O radical, formed by photolysis of CH_3ONO, than other alcoxy radicals. Table 6 shows a summary of the average yields of reaction products quantified for 4MCHexOH reactions.

Considering the products detected here and the those detected in the study of Bradley et al., (2001) relative to cyclohexanol with OH radical reactions, a degradation mechanism for 4MCHexOH with the atmospheric oxidants has been proposed. Figure 5A shows the paths that explain the formation of organic compounds (carbonyl, hydroxycarbonyl, etc), and Figure 5B shows an example of a path to explain the formation of nitrated organic compounds ($ROONO_2$ and $RONO_2$). Similar nitrated compounds could be formed by routes II−IV. The abstraction of hydrogen atom at the α−position with respect to OH group (route I) followed by the addition of oxygen, the formation of a peroxy radical and the fast decomposition of this radical explains the formation of E-4-methylcyclohexanone. Based on the molecular yield obtained for E-4-methylcyclohexanone for each oxidant (See Table 6), this route represents ~25/30%, ~40% and ~60% of the reaction mechanism of 4MCHexOH with Cl (absence/presence of NO_x), OH and NO_3, respectively. Percentages are two-fold higher than those predicted by the SARs method in the case of the Cl reactions and 1.3- and 1.5-fold lower for the OH and NO_3 reactions, respectively. These data should be taken with caution, since they could include many sources of error.

Apart from E-4-methylcyclohexanone, other carbonyl and hydroxycarbonyl compounds could be formed by routes II, III and IV. The presence of these types of compounds has been observed in the reactions with Cl and OH. According to the electron ionization mass spectra (EIMS) (Fig. S4, Supplementary Material) an assignation of peaks (C) and (D) shown in Fig. 3, to 2-hydroxy-5-methylcyclohexanone, 5-hydroxy-2-methylcyclohexanone and/or 3-methyl-1,6-hexanedial has been proposed. However, according to the atmospheric reactivity (Finlayson and Pitts, 2000; Calvert et al., 2011; Ziemann and Atkinson, 2012) and the study of Bradley et al. (2001), the compound that would be expected is 3-methyl-1,6-hexanedial, which arises from the decomposition of the alkoxy radical formed in route II. However, confirmation was not possible since these compounds are not commercially

available. The detection about 9% of HCOH in the reaction with Cl atoms indicates that the elimination of the methyl group in route IV is minor.

In the case of nitrate radical, the only carbonyl compound detected was E-4-methylcyclohexanone, suggesting that route I may be the dominant pathway for this radical. The large difference between the yields of E-4-methylcyclohexanone obtained using the SPME/GC-TOFMS system (~75%) or the FTIR (35%) could be due to the different methods of adding the precursor to the two reactors (small aliquots of N_2O_5 in the Teflon® reactor versus one large addition in the Pyrex® glass reactor). This procedure causes a lower initial concentration of nitrated inorganic species (NO_3, NO_2, HNO_3) in reactor of 150 L than in of 50 L reactor, favoring the formation of carbonyl compounds instead of nitrated organic compounds. Taking into account the yields of E-4-methylcyclohexanone and the nitrated compounds for the NO_3 reaction using FTIR analysis, a total carbon balance of 100% is obtained (See Table 6).

3.2.2. 3,3DM1ButOH

For the reaction of 3,3DM1ButOH with the three atmospheric oxidants, 3,3-dimethylbutanal was identified as the main reaction product. Figure S5A shows the FTIR spectra obtained for the reactions of 3,3DM1ButOH with Cl (absence/presence of NO_x), OH and NO_3. Residual FTIR spectra after subtraction of 3,3-dimethylbutanal (Fig. S5B), the SPME/GC-TOFMS chromatograms (Fig. S6) and the EIMS spectra (Fig. S7), show that other reaction products such as carbonyl, hydroxycarbonyl and nitrated compounds are formed. These reaction products could be formaldehyde, 2,2-dimethylpropanal, glycolaldehyde, acetone, and peroxy-3,3-dimethylbutyryl nitrate (P33DMBN) $(CH_3)_3CCH_2C(O)OONO_2$. These compounds can be formed as primary products (See Fig. 6) and/or secondary products from the degradation of 3,3-dimethylbutanal (See Fig. S8). The SPME/GC-TOFMS chromatograms show common peaks for the three oxidants, but the numbers of peaks and their distribution are very different, especially for OH reactions. In the case of the SPME/GC-TOFMS system, a set of experiment using field ionization was carried out in order to help establish the identification of reaction products.

Time–concentration profiles of 3,3DM1ButOH, 3,3-dimethylbutanal and those reaction products positively identified by FTIR analysis were made to test whether the profiles correspond to primary or secondary reaction products. An example of the reactions with Cl atoms in the absence and presence of NO_x is presented in Fig. 6, showing that in the absence of NO_x the profiles of acetone and formaldehyde have two trends. It indicates that these compounds are formed as primary and secondary products. This profile is clearly observed for nitrated compounds in the reaction with Cl atoms in the presence of NO_x (Fig. 6B).

A commercial sample of 3,3-dimethylbutanal was used to estimate the molecular yields in both experimental systems. These are shown in Table 4. The yields of acetone and formaldehyde were calculated using an FTIR reference spectrum of a commercial sample and FTIR reference spectra from Eurochamp database (https://data.eurochamp.org/data-access/spectra/), respectively. An FTIR reference spectrum of 2-methylpropanal (from this same database) was used to estimate the molecular yield of 2,2-dimethylpropanal.

The amounts of 3,3-dimethylbutanal formed were corrected by their reactions with Cl atoms, and with OH and NO_3 radicals using the rate coefficients available in literature or for reactions of structurally similar compounds (see footnote, Table 4). Estimated yields of formaldehyde, acetone, 2,2-dimethylpropanal and nitrated compounds are summarized in Table 6 along with an average yield of 3,3-dimethylbutanal. The higher yield of nitrated

compounds in the reaction of 3,3DM1ButOH with nitrate radical could indicate an extra formation of nitrated compounds from secondary reactions (See Fig. S8). Total of carbon yields of 60%, 81% and 36% have been justified for Cl, OH and NO_3 reactions respectively. It must be noted that there are reaction products that could not be quantified as dihydroxy or hydroxycarbonyl compounds in the reactions with Cl atoms in the absence of NO_x and primary nitrated compounds in the reactions with Cl atoms in the presence of NO_x and with NO_3 radical.

This work is the first study of the products of reaction of 3,3DM1ButOH with atmospheric oxidants, so there is no other study with which to compare. Figure 7 shows the reaction mechanism proposed based on literature studies of saturated alcohols reactions with Cl atoms and the OH radical (Cavalli et al., 2002; Hurley et al., 2009; McGillen et al., 2013; Welz et al., 2013) and considering the reaction products identified in our work. Table S2 in Supplementary Material, shows a summary of the reaction products, either observed or tentatively identified proposed in this mechanism of the reaction of 3,3DM1ButOH with the atmospheric oxidants.

As it can see in Table 4, the estimated molecular yields of 3,3-dimethylbutanal (formed by H atom abstraction at the α−position of 3,3DM1BuOH) are very similar to the one predicted by the SARs method for the Cl and OH reactions. In the case of NO_3 radical a large difference between yields was observed (36% estimated in this work, 86% predicted by SAR). This discrepancy could be explained by the fact that the SAR method applied to the NO_3 radical reaction with primary alcohols (Kerdouci et al., 2010, 2014) underestimates the attack of NO_3 at the β−position, since it does not consider the possible activating effect of the $-CH_2OH$ group (See S2, Supplementary Material). This could also explain the large difference observed between the estimated and measured rate coefficients of the reaction of 3,3DM1ButOH with NO_3 as shown in Table 2. On the other hand, the volume of the reactor could also have an influence on formation of 3,3-dimethylbutanal.

According to the molecular yields of the products quantified and/or observed in the SPME/GC-TOFMS chromatograms, it can be concluded that for the OH radical reaction, route I (attack at the α−position) seems to be the main reaction route. For Cl atoms the three routes can occur to a significant extent. The major molecular yields of formaldehyde and acetone (route III) in the reactions with Cl atoms in the presence of NO_x versus those of in the absence of NO_x could indicate that in the absence of NO_x the self reactions of peroxy radicals ($RO_2\cdot$) via the molecular pathway is more favored than via the radical pathway. For the NO_3 radical, routes I and II (attack at the β−position) with the formation of nitrated compounds seem to be the major routes.

3.2.3. 3,3DM2ButOH

Analysis of the FTIR spectra obtained for the reactions of 3,3DM2ButOH with Cl atoms in the presence and absence of NO_x, OH radical and NO_3 radical shows the formation of 3,3-dimethyl-2-butanone as a main product (see Fig. S9). Other compounds, such as formaldehyde, acetone, 2,2-dimethylpropanal and peroxyacetyl nitrate (PAN), were also observed. The residual FTIR spectra after subtraction of all known IR bands again shows the presence of carbonyl compounds (IR absorption in the range 1820−1700 cm^{-1}); hydroxy compounds (1060−1040 cm^{-1}) in the reaction with Cl atoms in the absence of NO_x, and also nitrated compounds ($RONO_2$; 1650, 1305−1260, 890 cm^{-1}) in the reaction with Cl in the presence of NO_x and NO_3 radical (Fig. S9C). The presence in the residual FTIR spectra of an IR absorption band around 1800 cm^{-1} for the reaction with Cl atoms at long reaction times could be due to the formation of chlorine compounds by reaction of 3,3-dimethyl-2-butanone with Cl_2 (Ren et al., 2018) or the formation of cyclic compounds such as hydrofurans. The SPME/GC-TOFMS

chromatograms and MS spectra (Fig. S10 and S11) confirm the presence of other reaction products apart from 3,3-dimethyl-2-butanone in the case of Cl (absence/presence of NO_x) and NO_3 reactions. Only one significant peak is observed in chromatograms of the OH reactions.

The estimated molecular yields of 3,3-dimethyl-2-butanone for all individual experiments are given in Table 5, where the measured concentrations have been corrected for secondary reactions. Acetone, formaldehyde, 2,2-dimethylpropanal, nitrated compounds and acetaldehyde were also quantified. Plots of concentration versus time for formaldehyde, acetone (Fig. S12A) and nitrated compounds in the reactions of Cl in the presence of NO_x (Fig. S12B) show profiles with two trends. This type of profile indicates that formaldehyde and acetone could also be formed by degradation of 3,3-dimethyl-2-butanone (Fig. S13). Table 6 summarizes the molecular yields of all quantified products.

Total carbon yields of ~60%/100%, 90% and 60% have been accounted for Cl (in the absence and presence of NO_x), OH and NO_3 reactions, respectively (See Table 6). It is important to note that in the case of the reaction of Cl atoms in the absence of NO_x, where the total carbon yield was lower than 100%, there were many reaction products that could not be quantified, such as dihydroxy and/or hydroxycarbonyl compounds. In the reaction with NO_3 radical, due to our experimental conditions, significant number of primary nitrated compounds was expected to be formed (Fig. S9C).

A mechanism of hydrogen atom abstraction at different positions on the carbon chain has been proposed for the reaction of 3,3DM2ButOH with Cl, OH and NO_3. The mechanism is shown in Figure 8. Table S3, in Supplementary Material, shows a summary of the reaction products either observed or tentatively identified proposed by this mechanism of the reactions of 3,3DM2ButOH with the atmospheric oxidants.

Molecular yields of 3,3-dimethyl-2-butanone obtained in this work imply percentages of attack of the oxidant at the α−position (route II) of: 43%/44% in the case of Cl atom (absence/presence of NO_x); 81% for the OH radical and 58% for the NO_3 radical. Percentages are very similar to those predicted by SARs except for the NO_3 radical (See Table 5). High NO_2 concentration present in the reactions with NO_3 radical would greatly favor the formation of nitrated compounds over 3,3-dimethyl-2-butanone. It could justify the low estimated molecular yield for 3,3-dimethyl-2-butanone.

The main reaction products observed in the reaction with Cl atoms in the presence of NO_x (3,3-dimethyl-2-butanone, formaldehyde, 2,2-dimethylpropanal, acetone and acetaldehyde) confirm the attack of Cl atoms at other sites apart from the α−position. Based on the estimated molecular yield of acetone, attack at the δ−position with abstraction of hydrogen atom from methyl groups (route III) could be ~58%, and based on the estimated molecular yield of 2,2-dimethylpropanal, the attack at the β−position (route I) could account for 10%. These data agree with the SAR predictions for Cl atom reactions. On the other hand, the major molecular yields of acetone, formaldehyde and acetaldehyde (route III) in the reaction with Cl atoms in the presence of NO_x rather than in its absence could indicate that in the presence of NO_x the self-reactions of peroxy radicals via the molecular pathway is negligible. The lower yield estimated (17 %) of acetaldehyde versus 58% of its coproduct (acetone) is due to its fast degradation by reaction with Cl atoms with the formation PAN as observed in the FTIR experiments (See Fig. S9B).

4. Atmospheric Implications

1 Pollutants in the atmosphere, can create serious environmental problems, such photochemical smog, acid rain and

2 degradation of the ozone layer (Finlayson-Pitts and Pitts, 2000). So, it is important to evaluate the parameters that

3 help us to understand the impact of the presence of these compounds in the atmosphere. These parameters are the

4 time that such compounds remain in the atmosphere, their global warming potential (GWP) and their mechanisms

5 of degradation, in order to estimate the atmospheric effect of products formed.

6 The first important parameter of the environmental impact of oxygenated volatile organic compounds in the

7 atmosphere is the global lifetime, τ_{global}, which considers all the degradation processes that could affect these

8 compounds in the troposphere. This parameter can be obtained from the sum of the individual sink processes such

9 as reactions initiated by OH and NO_3 radicals, Cl atoms, and O_3 molecules; photolysis and dry and wet deposition,

10 Eq (4):

$$\tau_{global} = \left[\frac{1}{\tau_{OH}} + \frac{1}{\tau_{Cl}} + \frac{1}{\tau_{NO_3}} + \frac{1}{\tau_{O_3}} + \frac{1}{\tau_{photolysis}} + \frac{1}{\tau_{other\ processes}}\right]^{-1} \tag{4}$$

12 The tropospheric lifetime (τ) of 4MCHexOH, 3,3DM1ButOH and 3,3DM2ButOH for each process have been

13 estimated by considering Eqs (4) and (5):

$$\tau = \frac{1}{k_{Ox}[Ox]} \tag{5}$$

15 where k_{OX} and [Ox] are the rate coefficients obtained in this work for each oxidant and the typical atmospheric

16 concentrations of the oxidants Cl, OH and NO_3, respectively. Concentrations employed were as follows: for 24 h

17 average: 1×10^3 atoms cm^{-3} (Platt and Janssen, 1995) for Cl, 12 h average daytime concentration of 1×10^6

18 radicals cm^{-3} for OH (Prinn et al., 2001) and 5×10^8 radicals cm^{-3} for NO_3 (Atkinson, 2000), and a peak

19 concentration of Cl of 1.3×10^5 atoms cm^{-3} in the coastal marine boundary layer at dawn (Spicer et al., 1998).

20 Reactions with O_3 and photolysis are negligible loss processes for this type of compound (Mellouki et al., 2015).

21 Other processes are referred to as dry and wet deposition. To estimate the lifetime associated with wet deposition,

22 Eq (6) proposed by (Chen et al. 2003) was used:

$$\tau_{wet} = \frac{H_{atm}}{v_{pm}RTk_H} \tag{6}$$

24 where k_H is the Henry's law constant, H_{atm} is the height of the troposphere, taking a value of 630 m, v_{pm} is the

25 average precipitation rate for Ciudad Real (Spain) (402 mm yr^{-1}) (www.aemet.es), R is the gas constant and T is

26 the temperature, considered to be constant and equal to 298 K. In the literature there are only data of Henry's

27 constant for 3,3DM2ButOH (5.6×10^{-1} mol m^{-3} Pa^{-1}) (Sander, 2015). Comparing the available data for similar

28 compounds approximated values of K_H of 3 mol m^{-3} Pa^{-1} and 0.4 mol m^{-3} Pa^{-1} for 4MCHexOH and

29 3,3DM1ButOH, respectively have been used.

30 The calculated lifetimes of the three alcohols studied in this work are shown in Table 7. It can be seen that the

31 dominant tropospheric loss process for the three alcohols is clearly their reaction with OH radicals followed by

32 their reaction with NO_3 radicals at night. However, in places where there is a peak concentration of chlorine atoms

33 (coastal areas) the reaction of these alcohols with chlorine atoms may compete with that with OH radicals as their

34 main degradation process.

35 The global lifetime of the three alcohols is of the order of ~ 1−2 days, indicating that these compounds will

36 probably be degraded near their sources. These global lifetimes also indicate that SAs do not make a significant

contribution to the radiative forcing of climate change (Mellouki et al., 2015), which is supported through the estimation of their GWP values. For a time-horizon of 20 years, the estimated values are: 8.33×10^{-4}, 1.78×10^{-2} and 5.80×10^{-3} for 4MCHexOH, 3,3DM1ButOH and 3,3DM2ButOH respectively, which are very low. So, these compounds will only have an important impact in the troposphere at a local or regional level.

Their degradation products (mostly carbonyl-containing compounds and nitro-compounds in polluted areas) must be considered. Thus, the nitrated compounds generated can act as NOx reservoir species especially during the night (Altshuller, 1993) and could have an influence at the global scale. Moreover, since 4MCHexOH, 3,3DM1ButOH and 3,3DM2ButOH react quickly with Cl atoms and OH radicals, their contribution to the formation of photochemical smog might be important. For that reason, the contribution of these three alcohols to the formation of smog was estimated by obtaining the average ozone production during 99% of their reactions with OH radical, using the equation indicated by Dash and Rajakumar (2013). The values obtained were 3.24, 0.90 and 1.69 ppm for 4MCHexOH, 3,3DM1ButOH and 3,3DM2ButOH, respectively. These values suggest that these compounds may be potential generators of tropospheric ozone and could contribute significantly to the formation of photochemical smog depending on their concentrations in the atmosphere.

5. Conclusions

The main conclusions obtained from the present study, are the following:

− The kinetic and product study support that: 1 − The atmospheric degradation mechanism for SAs, and possibly for other unstudied saturated alcohols, proceeds by abstraction of a hydrogen atom bonded to a carbon rather than a hydrogen atom bonded to the oxygen atom of the alcohol group, and 2 − The reaction mechanism in the H atom abstraction process depends on the oxidant. Cl atoms abstract any type of hydrogen (α, β, δ) from SAs with a high percentage compared to the OH and the NO_3 radicals. The OH and NO_3 radicals abstract mainly the hydrogen atom at the α−position, if the saturated alcohols are secondary. For primary alcohols, the abstraction of a hydrogen atom at the β−position could also be important in the reaction with NO_3 radical. Therefore, more kinetic studies of the NO_3 radical reaction with primary alcohols are necessary to quantify the effect of the OH group at the β−position ($-CH_2OH$) and to update the SAR method developed by Kerdouci et al.

− Theoretical ab-initio studies of the reactions of SAs with atmospheric oxidants should be performed in order to obtain more information about their reaction mechanisms in the H atom abstraction process.

− The atmospheric conditions determine the reaction mechanism and therefore the reaction products obtained in the degradation of SAs. So, in polluted environments with high concentrations of NOx, the peroxy radicals react mainly with NO to form the alkoxy radical instead of molecular compounds. In these conditions, nitrated organic compounds ($RONO_2$) are formed as well as polyfunctional organic compounds. Also, when the concentration of NO_2 is higher than that of NO, ozone is formed. In a clean atmosphere, as in the case of the experiments with Cl atoms in the absence of NO_x, the reaction products are different because, peroxy radicals could react mainly via a self-reaction molecular pathway instead of via a self-reaction radical pathway with formation of dihydroxy and hydroxycarbonyl compounds.

− The unquantified polyfunctional organic compounds could explain the low carbon balance obtained in the Cl or NO_3 reactions. The carbon balance must be taken with caution since the calculated molecular yields have a high degree of uncertainty.

- Calculated lifetimes for saturated alcohols (in the order of ~1 day) imply that these compounds are pollutants at a local–regional scale, but it is also important to indicate that SAs are sources of stable nitrated compounds ($ROONO_2$), depending on environmental conditions, that can travel large distances from their sources and contribute to form ozone in clean areas, for example in forest or rural areas.

- The main products of the degradation of the SAs, aldehydes and ketones, develop a very important secondary chemistry with the formation of products of special relevance, such as the PAN observed in the degradation of 3,3-dimethyl-2-butanol. More experiments should be carried out using other detection techniques in order to evaluate the formation of secondary organic aerosol (SOA) because it is well known that polyfunctional organic compounds are important SOA precursors.

- From the environmental point of view, this work shows that the degradation of SAs is an important source of pollutants in the atmosphere of greater or lesser impact depending on the environmental conditions and the quantities of these alcohols present in the atmosphere. Therefore, the use of SAs as additives in the production of biofuels should be controlled, as poor handling could result in high concentrations of these alcohols in the atmosphere.

- The rate coefficients and reaction products reported in this work are the first available data, so this work contributes to a better understanding of the atmospheric chemistry of oxygenated compounds, expands the kinetic and mechanistic database, and contributes to developing or to improving predictive models that help us to avoid or mitigate the effects of climate change or air quality. However, kinetic experiments in the tropospheric temperature range are necessary to obtain more information about the reaction mechanism and to extrapolate the rate coefficient data to other typical atmospheric conditions and thus be able to better establish the atmospheric impact of these alcohols.

6. Supplementary material.

Attached in a separated file.

7. Data availability.

The underlying research data are available on request by email to the contact author of this work.

8. Author contribution

Salgado S. and Martín P. designed the experiments. Cabañas B. is the leader of the group and the responsible to control the research and got the financial support for the project leading to this publication. Colmenar I. carried out the experiments of 4MCHexOH. Tapia A. carried out the kinetic experiments of 3,3DM1ButOH and 3,3DM2ButOH and Aranda I. carried out the product experiments of 3,3DM1ButOH and 3,3DM2ButOH. Martín P. supervised all analysis of data and prepared the manuscript with contributions from all co-authors.

9. Competing interests

The authors declare that they have no conflict of interest.

10. Acknowledgment

11. References

-Allert, M., Rizk, S. S., Looger, L. L., Hellinga, H. W., and Wells, J.. A Computational Design of Receptors for an Organophosphate Surrogate of the Nerve Agent Soman. *Proc. Natl. Acad. Sci.* 101, 21. 7907-7912, https://doi.org/10.1073/pnas.0401309101, 2004.

-Altshuller A. P. PANs in the Atmosphere, *Air & Waste*, 43:9, 1221-1230, https://doi.org/10.1080/1073161X.1993.10467199, 1993.

-Andersen, V. F., Wallington, T. J., Nielsen, O. J. Atmospheric Chemistry of i-Butanol. *J. Phys. Chem. A*., 114, 12462−12469, https://doi.org/10.1021/jp107950d, 2010.

-AOPWIN, v1.92. ©2000 U.S. Environmental Protection Agency.

-Aschmann, S. M. Arey, J. and Atkinson R. Kinetics and Products of the Reactions of OH Radicals with 4,4-Dimethyl-1-pentene and 3,3-Dimethylbutanal at 296 ±2 K. *J. Phys. Chem. A,* 114, 5810–5816, https://doi.org/10.1021/jp101893g, 2010.

-Atkinson, R. Gas-phase tropospheric chemistry of organic compounds. *J. Phys. Chem. Ref. Data*. Monograph, 1-216, 1994.

-Atkinson, R. Atmospheric chemistry of VOCs and NO(x). *Atmos. Environ*. 34(12-14), 2063-2101, https://doi.org./10.1016/S1352-2310(99)00460-4, 2000.

-Atkinson, R. Kinetics of the gas-phase reactions of OH radicals with alkanes and cycloalkanes. *Atmos. Chem. Phys.* 3, 2233-2307, https://doi.org/10.5194/acp-3-2233-2003, 2003.

-Atkinson, R. and Arey J. Atmospheric degradation of volatile organic compounds. *Chem Rev* 103:4605–4638, https://doi.org/10.1021/cr0206420, 2003.

-Atkinson, R., Aschmann, S.M., Pitts Jr., J.N. Rate constants for the gas-phase reactions of the NO_3 radical with a series of organic compounds at 296 ± 2 K. *J. Phys. Chem*. 92, 3454-3457, https://doi.org/10.1021/j100323a028, 1988.

-Atkinson, R., Aschmann, S.M., Pitts Jr. J.N. Rate Constants for the Gas-Phase Reactions of the OH Radical with a Series of Aromatic Hydrocarbons at 296 ± 2 K. *Int. J.Chem. Kinet*. 21, 355-365, https://doi.org/10.1002/kin.550210506, 1989.

-Atkinson, R., Baulch, D. L., Cox, R. A., Crowley, J. N., Hampson, R. F., Hynes, R. G., Jenkin, M. E., Rossi, M. J., Troe, J., and IUPAC Subcommittee. Evaluated kinetic and photochemical data for atmospheric chemistry: Volume II – gas phase reactions of organic species, *Atmos. Chem. Phys,* 6, 3625-4055, https://doi.org/10.5194/acp-6-3625-2006, 2006.

-Atkinson, R., Plum, C.N., Carter, W.P.L., Winer, A.M., Pitts Jr. J.N. Rate constants for the gas-phase reactions of nitrate radicals with a series of organics in air at 298 ± 1 K. *J. Phys. Chem.* 88, 1210-1215, https://doi.org/10.1021/j150650a039, 1984.

-Ballesteros, B., Garzón, A., Jiménez, E., Notario, A., Albaladejo, J. Relative and absolute kinetic studies of 2-butanol and related alcohols with tropospheric Cl atoms *J. Phys. Chem. Chem. Phys.* 9 (10), 1210-1218, https://doi.org/10.1039/B614531K, 2007.

-Bradley, W.R., Wyatt, S.E., Wells, J.R., Henley, M.V., Graziano, G.M.The Hydroxyl Radical Reaction Rate Constant and Products of Cyclohexanol. *Int. J. Chem. Kinet.*, 33, 108-117, https://doi.org/10.1002/1097-4601(200102)33:2<108::AID-KIN1002>3.0.CO;2-%23, 2001.

-Brauers, T., Finlayson-Pitts, B.J. Analysis of relative rate measurements. *Int. J. Chem. Kinet.* 29 (9), 665-672, https://doi.org/10.1002/(SICI)1097-4601(1997)29:9<665::AID-KIN3>3.0.CO;2-S, 1997.

-Calvert, J.G., Mellouki, A., Orlando, J.J., Pilling, M.J., Wallington, T.J. The mechanisms of atmospheric oxidation of the oxygenates. Oxford University Press, New York, 2011.

-Caravan, R. L., Shannon, R. J., Lewis, T., Blitz, M. A., and Heard, D. E. Measurements of Rate Coefficients for Reactions of OH with Ethanol and Propan-2-ol at Very Low Temperatures. *J. Phys. Chem. A,* 119, 7130−7137, https://doi.org/10.1021/jp505790m, 2015.

-Cavalli, F., Geiger, H., Barnes, I., Becker, K. H. FTIR Kinetic, Product, and Modeling Study of the OH-Initiated Oxidation of 1-Butanol in Air. *Environ. Sci. Technol.*, 36, 1263−1270, https://doi.org/10.1021/es010220s, 2002.

-Ceacero-Vega, A. Ballesteros, B., Albaladejo, J., Bejan, I., and Barnes, I. Temperature dependence of the gas-phase reactions of Cl atoms with propene and 1-butene between $285 < T < 313$ K. *Chem. Phys.Lett.* 484(1-3):10–13, https://doi.org/10.1016/j.cplett.2009.10.080, 2009.

-Ceacero-Vega, A.A., Ballesteros, B., Bejan, I., Barnes, I., Jiménez, E., Albaladejo, J. Kinetics and Mechanisms of the Tropospheric Reactions of Menthol, Borneol, Fenchol, Camphor, and Fenchone with Hydroxyl Radicals (OH) and Chlorine Atoms (Cl). *J. Phys. Chem, A.*, 116, 4097-4107, https://doi.org/10.1021/jp212076g, 2012.

-Chen, L., Takenaka N., Bandow, H. Maeda, Y. Henry's law constants for C2–C3 fluorinated alcohols and their wet deposition in the atmosphere. *Atmos. Environ.* 37, 34,4817-4822, https://doi.org/10.1016/j.atmosenv.2003.08.002, 2003.

-Cheung C.S., Huang Z. Effect of n-pentanol addition on the combustion, performance and emission characteristics of a direct-injection diesel engine. *Energy*; 70:172–80, https://doi.org/10.1016/j.energy.2014.03.106, 2014.

-D'Anna, B., Andresen, W., Gefen, Z., Nielsen, C.J. 2001. Kinetic study of OH and NO_3 radical reactions with 14 aliphatic aldehydes. *Phys. Chem. Chem. Phys.* 3, 15, 3057-3063, https://doi.org/10.1039/B103623H, 2001.

-Dash, M.R. and Rajakumar, B. Experimental and theoretical rate coefficients for the gas phase reaction of β-Pinene with OH radical. *Atmos. Environ,* 79, 161-171, https://doi.org/10.1016/j.atmosenv.2013.05.039, 2013.

-Ezzel, M.J., Wang, W., Ezell, A.A., Soskin, G., Finlayson- Pitts, B.J. **2002**. Kinetics of reactions of chlorine atoms with a series of alkenes at 1 atm and 298 K: structure and reactivity. *Phys. Chem. Chem. Phys.*, 1, 5813-5820, https://doi.org/10.1039/B207529F, 2002.

-Farrugia, L.N., Bejan, I., Smith, S.C., Medeiros, D.J., Seakins, P.W. Revised structure activity parameters derived from new rate coefficient determinations for the reactions of chlorine atoms with a series of seven ketones at 290 K and 1 atm. *Chem. Phys. Lett.* 640 87–93, https://doi.org/10.1016/j.cplett.2015.09.055, 2015.

-Finlayson-Pitts, B. J. and Pitts, J.N. Chemistry of the Upper and Lower Atmosphere: Theory, Experiments, and Applications" Academic Press, San Diego, 2000.

-Gallego-Iniesta, M.P., Moreno, A., Martín, P., Tapia, A., Cabañas, B., Salgado. M.S. Reactivity of 2-ethyl-1-hexanol in the atmosphere. *Phys. Chem. Chem. Phys.* 12, 3294-3300, https://doi.org/10.1039/B923899A, 2010.

-Gallego-Iniesta, M.P., Cabañas, B., Salgado. M.S. Martinez, E., Martin, P. Estimation of gas-phase rate coefficients for the reactions of a series of α,β−unsaturated esters with OH, NO_3, O_3 and Cl. *Atmos. Environ.* 90, 133-145, https://doi.org/10.1016/j.atmosenv.2014.03.036, 2014.

-Garzón, A., Cuevas, C.A., Ceacero, A.A. ,Notario, A., Albaladejo, J. and Fernández-Gómez, M. Atmospheric reactions Cl +CH3 –(CH$_2$)$_n$–OH (n=0-4): A kinetic and theoretical study. *J. Chem. Phys.*125., 104305-104315, https://doi.org/10.1063/1.2244556, 2006.

-Grosjean, D. Atmospheric chemistry of alcohols. *J. Braz. Chem. Soc*. 8, 433-442, http://dx.doi.org/10.1590/S0103-50531997000500002, 1997.

-Herath, N.T., Orozco, I., Clinch, E.C., Marshall, P. Relative Rate Studies of the Reactions of Atomic Chlorine with Acetone and Cyclic Ketones. *Int. J. Chem. Kinet.* 50, 41-46, https://doi.org/10.1002/kin.21138, 2018.

-Hurley, M. D., Wallington, T. J., Laursen, L., Javadi, M. S., Nielsen, O. J., Yamanaka, T., Kawasaki, M. Atmospheric Chemistry of n-Butanol: Kinetics, Mechanisms, and Products of Cl Atom and OH Radical Initiated Oxidation in the Presence and Absence of NOx. *J. Phys. Chem. A*, 113, 7011−7020, https://doi.org/10.1021/jp810585c, 2009.

-Jenkin, M.E., Valorso, R., Aumont, B., Rickard, A.R., Wallington, T.J. Estimation of rate coefficients and branching ratios for gas-phase reactions of OH with aliphatic organic compounds for use in automated mechanism construction. *J. Atmos. Chem. Phys*. 18, 9297-9328, https://doi.org/10.5194/acp-18-9297-2018, 2018.

-Jiménez. E., Lanza, B., Garzón, A., Ballesteros, B., Albaladejo, J. Atmospheric Degradation of 2-Butanol, 2-Methyl-2-butanol, and 2,3-Dimethyl-2-butanol: OH Kinetics and UV Absorption Cross Sections. *J. Phys. Chem. A*.109, 10903-10909, https://doi.org/10.1021/jp054094g, 2005.

-Karabektas, M. and Hosoz, M. Performance and emission characteristics of a diesel engine using isobutanol–diesel fuel blends, *Renew Energy*, 34 (6), 1554-1559, https://doi.org/10.1016/j.renene.2008.11.003, 2009.

-Kerdouci, J., Picquet-Varrault, B., Doussin, J.F. Prediction of Rate Constants for Gas-Phase Reactions of Nitrate Radical with Organic Compounds: A New Structure–Activity Relationship. *Chem. Phys.Chem.*, 11, 3909-3920, https://doi.org/10.1002/cphc.201000673, 2010.

-Kerdouci, J., Picquet-Varrault, B., Doussin, J.F. Structure–activity relationship for the gas-phase reactions of NO$_3$ radical with organic compounds: Update and extension to aldehydes. *Atmos. Environ*. 84, 363-372, https://doi.org/10.1016/j.atmosenv.2013.11.024, 2014.

-Kumar., B.R. and Saravanan, S. Use of higher alcohol biofuels in diesel engines: A review. *Renew. Sust. Energ. Rev.* 60, 84–115, https://doi.org/10.1016/j.rser.2016.01.085, 2016.

-Kwok, E.S.C. and Atkinson R. Estimation of Hydroxyl Radical Reaction Rate Constants For Gas-Phase Organic Compounds Using A Structure-Reactivity Relationship: An Update. *Atmos. Environ.,* 29, 1685-1695, https://doi.org/10.1016/1352-2310(95)00069-B, 1995.

-Lapuerta, M., García-Contreras, R., Campos-Fernández, J., and Dorado P. Stability, lubricity, viscosity, and cold-flow properties of alcohol−diesel blends, *Energy Fuels*, 24, 4497-4502, https://doi.org/10.1021/ef100498u, 2010.

-Li, F., Yi, B., Song, L., Fu, W., Liu, T., Hu, H., & Lin, Q. Macroscopic spray characteristics of long-chain alcohol-biodiesel fuels in a constant volume chamber. Proceedings of the Institution of Mechanical Engineers, Part A: *JPE*, 232(2), 195−207. https://doi.org/10.1177/0957650917721336, 2017.

-Lopes, M., Serrano, L., Ribeiro, I., Cascao, P., Pires, N. Emissions characterization from EURO 5 diesel/biodiesel passenger car operating under the new European driving cycle. *Atmos. Environ.* 84, 339-348, https://doi.org/10.1016/j.atmosenv.2013.11.071, 2014.

- Martin, P., Cabañas, B., Colmenar, I., Salgado, M.S., Villanueva, F., Tapia, A. Reactivity of E-butenedial with the major atmospheric oxidants. *Atmos. Environ.* 70, 351-360, https://doi.org/10.1016/j.atmosenv.2013.01.041, 2013

- McGillen, M. R., Baasandorj, M., Burkholder, J. B. Gas-Phase Rate Coefficients for the OH + n-, i-, s-, and t-Butanol Reactions Measured Between 220 and 380 K: Non-Arrhenius Behavior and Site- Specific Reactivity. *J. Phys. Chem. A*, 117, 4636−4656, https://doi.org/10.1021/jp402702u, 2013.

-McGillen, M.R., Tyndall, G.S., Orlando, J.J, Pimentel, A.S., Medeiros, D.J., and Burkholder J.B. Experimentally Determined Site-Specific Reactivity of the Gas-Phase OH and Cl + i-Butanol Reactions Between 251 and 340 K. *J. Phys. Chem. A*, 120, 9968−9981, https://doi.org/10.1021/acs.jpca.6b09266, 2016.

-Mellouki, A., Wallington, T. J., Chen, J. Atmospheric chemistry of oxygenated volatile organic compounds: impacts on air quality and climate. *Chem Rev*., 115:3984–4014, https://doi.org/10.1021/cr500549n, 2015.

-Moc, J and Simmie, J.M. Hydrogen Abstraction from n-Butanol by the Hydroxyl Radical: High Level Ab Initio Study of the Relative Significance of Various Abstraction Channels and the Role of Weakly Bound Intermediates. *J. Phys. Chem. A,* 114, 5558–5564, https://doi.org/10.1021/jp1009065, 2010.

-Moreno, A., Salgado, S., Martin, P., Martinez, E., and Cabañas, B. Kinetic Study of the Gas Phase Reactions of a Series of Alcohols with the NO_3 Radical. *J. Phys. Chem. A*, 116, 42, 10383-10389, https://doi.org/10.1021/jp305682h, 2012.

-Moreno, A., Salgado, S., Taccone, R., Martín, P., Cabañas, B. Atmospheric degradation of saturated alcohols: room temperature rate coefficients for NO_3 radical reactions. *Atmos. Environ*., 96, 229-235, https://doi.org/10.1016/j.atmosenv.2014.07.037, 2014.

-Murty, M. R. V. S, Prasada, R. N., Prabhakar, S., and Vairamani, M. Chemical ionization mass spectral analysis of pinacolyl alcohol and development of derivatization method using p-tolyl isocyanate. *Anal Methods* 2:1599–1605, https://doi.org/10.1039/C0AY00346H, 2010.

-Nelson, L., Rattigan, O., Neavyn, R., Sidebottom, H., Treacy, J., Nielsen, O. J. Absolute and Relative Rate Constants for the Reactions of Hydroxyl Radicals and Chlorine Atoms with a Series of Aliphatic Alcohols and Ethers at 298 K. *Int. J. Chem. Kinet*., 22, 1111− 1126. https://doi.org/10.1002/kin.550221102, 1990.

-Nguyen, H.T., Takenaka, N., Bandow, H., Maeda, Y., Oliva, S.T., Botelho, M.M. and Tavares T.M. Atmospheric alcohols and aldehydes concentrations measured in Osaka, Japan and in Sao Paulo, Brazil. *Atmos. Environ,* 35, 3075-3083. https://doi.org/10.1016/S1352-2310(01)00136-4, 2001.

-Ozsezen, N. A., Turkcan, A., Sayin, C. and Canakci, M. Comparison of performance and combustion parameters in a heavy-duty diesel engine fueled with iso-butanol/diesel fuel blends. *Energy. Explor. Exploit*, 29, 525-541, https://doi.org/10.1260/0144-5987.29.5.525, 2011.

-Poutsma, M. L. Evolution of Structure−Reactivity Correlations for the Hydrogen Abstraction Reaction by Chlorine Atom *J. Phys. Chem. A*, 117(4), 687–703. https://doi.org/10.1021/jp310970t, 2013.

-Platt U. and Janssen C. 1995. Observation and role of the free radicals NO_3, ClO, BrO and IO in the troposphere. *Faraday Discussions.* https://doi.org/100:175-198,10.1039/FD9950000175, 1995.

-Prinn, R.G., Huang, J., Weiss, R.F., Cunnold, D.M., Fraser, P.J., Simmonds, P.G., McCulloch, A., Harth, C., Salameh, P., O'Doherty, S., Wang, R.H.J., Porter, L., Miller, R.B. Evidence for Substantial Variations of Atmospheric Hydroxyl Radicals in the Past Two Decades *Science* 292, 1882-1888, https://doi.org/10.1126/science.1058673, 2001.

1 -Ren, Y., Huang, Z., Miao, H., Di, Y., Jiang, D., Zeng, K., Liu, B., Wang, X. Combustion and emissions of a DI

2 diesel engine fuelled with diesel-oxygenate blends, *Fuel*, 87, 2691-2697,

3 https://doi.org/10.1016/j.fuel.2008.02.017, 2008.

4 -Ren Y. Wang J. Grosselin B. Daele V. and Mellouki A. Kinetic and product studies of Cl atoms reactions with a

5 series of branched ketones. *J. Environ. Science.* 71, 271-282, https://doi.org/10.1016/j.jes.2018.03.036, 2018.

6 -Sander, R. Compilation of Henry's law constants (version 4.0) for water as solvent *Atmos. Chem. Phys,* 15, 8,

7 4399-4981, https://doi.org/10.5194/acp-15-4399-2015, 2015.

8 -Sarathy, M., Oßwald P., Hansen, N., and Kohse-Höinghaus, K. Alcohol combustion chemistry. *Prog. Energy*

9 *Combust. Sci*. 44. 40-102, https://doi.org/10.1016/j.pecs.2014.04.003, 2014.

10 -Schott, G., and Davidson, N. Shock Waves in Chemical Kinetics: The Decomposition of N_2O_5 at High

11 Temperatures, *J. Am. Chem. Soc*., 80, 1841-1853, https://doi.org/10.1021/ja01541a019, 1958.

12 -Sikarwara, V.S, Zhao M., Fennell, P.S., Shah, N., Anthony, E.J. Progress in biofuel production from gasification.

13 *Prog. Energ. Combust.* 61, 189-248, https://doi.org/10.1016/j.pecs.2017.04.001, 2017.

14 -Smith, I. W. M., Ravishankara, A. R. J. Role of Hydrogen-Bonded Intermediates in the Bimolecular Reactions

15 of the Hydroxyl Radical. *Phys. Chem. A*, 106, 4798-4807, https://doi.org/10.1021/jp014234w, 2002.

16 -Spicer, C., Chapman, E.G., Finalysson-Pitts, B.J., Plastridege, R.A., Hybbe, J.M., Fast, J.D., Berkowitz, C.M.

17 Unexpectedly high concentrations of molecular chlorine in coastal air *Nature*, 394, 353–356,

18 https://doi.org/10.1038/28584, 1998.

19 -Tapia, A., Villanueva, F., Salgado, S., Cabañas, B., Martinez, E. and Martin, P. Atmospheric degradation of 3-

20 methylfuran: kinetic and products study. *Atmos. Chem. Phys.,* 2011, 11, 3227–3241. https://doi.org/10.5194/acp-

21 11-3227-2011.

22 -Taylor, W.D., Alston, T.D., Moscato, M.J., Fazekas, G.B., Kozlowski, R., Takacs, G.A Atmospheric

23 photodissociation lifetimes for nitromethane, methyl nitrite, and methyl nitrate. *Int. J. Chem. Kinet*. 12, 231-240,

24 https://doi.org/10.1002/kin.550120404, 1980.

25 -Thevenet, R., Mellouki, A., Bras, G. L. Kinetics of OH and Cl Reactions with a Series of Aldehydes. *Int. J. Chem.*

26 *Kinet.,* 32, 676–685, https://doi.org/10.1002/1097-4601(2000)32:11<676::AID-KIN3>3.0.CO;2-V, 2000.

27 -Tuazon E. C. and Atkinson, R. A Product Study of the Gas-Phase Reaction of Isoprene with the OH Radical in

28 the Presence of NOx. *Int. J. Chem. Kinet*. 22, 1221-1236, https://doi.org/10.1002/kin.550221202, 1990.

29 -Tuazon E. C., Leod, H.M, Atkinson, R. and Carter W.P.L. α-Dicarbonyl Yields from the NO_x Air Photooxidations

30 of a Series of Aromatic Hydrocarbons in Air. *Environ. Sci. Technol.,* 20, 4, 383-387,

31 https://doi.org/10.1021/es00146a010, 1986.

32 -Vereecken, L., Aumont, B., Barnes, I., Bozzelli, J.W., Goldman, M.J., Green, W.H., Madronich, S., Mcgillen,

33 M.R., Mellouki, A., Orlando, J. J., Picquet-Varrault, B., Rickard, R., Stockwell, W. R., Wallington, T.J., Carter,

34 W.P.L. Perspective on Mechanism Development and Structure-Activity Relationships for Gas-Phase Atmospheric

35 Chemistry. *Int. J. Chem. Kinet.* 50, 435-469, http://dx.doi.org/10.1002/kin.21172, 2018.

36 -Wallington, T.J. and Kurylo, M.J. Flash Photolysis Resonance Fluorescence Investigation of the Gas-Phase

37 Reactions of OH Radicals with a Series of Aliphatic Ketones over the Temperature Range 240-440 K. *J. Phys.*

38 *Chem.*, 91, 19, 5050-5054, https://doi.org/10.1021/j100303a033, 1987.

-Wallington, T.J., Skwes, L.M., Siegl, W.O, Wu. C., Japar, S.M. Gas phase reaction of Cl atoms with a series of oxygenated organic species at 295 K, *Int. J. Chem. Kinet*., 20, 867-875, https://doi.org/10.1002/kin.550201105, 1988.

-Wayne R.P., Barnes I., Biggs P., Burrows J.P., Canosa-Mas C.E., Hjorth J., LeBras G., Moortgat G.K., Perner D., Poulet G., Restelli G., Sidebottom H. The nitrate radical: Physics, chemistry, and the atmosphere. *Atmos. Environ.,* 25A, 1-203, https://doi.org/10.1016/0960-1686(91)90192-A, 1991.

-Wayne, R.P. Chemistry of Atmospheres. Oxford University Press, New York, 2000.

-Welz,O., Klippenstein, S., O., J., Harding, L. B., Taatjes, C. A., Zádor, J. Unconventional Peroxy Chemistry in Alcohol Oxidation: The Water Elimination Pathway. *J. Phys. Chem. Lett*., 43, 350-354, https://doi.org/10.1021/jz302004w, 2013.

-Ziemann P., and Atkinson R. Kinetics, products, and mechanisms of secondary organic aerosol formation. *Chem Soc Rev*. 41(19), 6582-6605, https://doi.org/10.1039/C2CS35122F, 2012.

-www.aemet.es
-www.capotchem.com
-www.iea.org. Energy and Air Pollution. World Energy Outlook 2016 Special Report Workshop International Energy Agency.
-www.iupac-kinetic.ch.cam.ac.uk IUPAC Subcommittee on Gas Kinetic Data Evaluation.
-www.thermofisher.com/search/browse/results?customGroup=Spectral+Libraries)
-webbook.nist.gov/chemistry/
-https://data.eurochamp.org/data-access/spectra/

Table 1. Rate coefficient ratios, absolute rate coefficients and average rate coefficients for the reactions of a series of SAs with Cl atoms and OH and NO_3 radicals at 298 K and 720 ± 20 Torr of pressure. Rate coefficients, k, in cm^3 molecule^{-1} s^{-1}.

Reaction	Reference	$(k_{SA}/k_R) \pm 2\sigma$	$(k_{SA} \pm 2\sigma)^a/10^{-10}$	$(\overline{k}_{SA} \pm 2\sigma)^b/10^{-10}$
3,3DM1ButOH + Cl	1-butene	0.85 ± 0.03	2.89 ± 0.42	2.69 ± 0.16
		0.79 ± 0.02	2.68 ± 0.38	
		0.76 ± 0.02	2.58 ± 0.37	
	Propene	1.18 ± 0.02	2.63 ± 0.37	
		1.21 ± 0.03	2.70 ± 0.38	
		1.22 ± 0.03	2.71 ± 0.38	
3,3DM2ButOH + Cl	1-butene	0.42 ± 0.01	1.42 ± 0.21	1.21 ± 0.07
		0.35 ± 0.01	1.17 ± 0.17	
		0.41 ± 0.01	1.38 ± 0.20	
	Propene	0.48 ± 0.01	1.08 ± 0.15	
		0.50 ± 0.02	1.12 ± 0.16	
		0.56 ± 0.03	1.26 ± 0.19	
4MCHexOH + Cl	2-methylpropene	1.08 ± 0.03	3.69 ± 0.32	3.70 ± 0.16
		1.16 ± 0.02	3.95 ± 0.33	
		0.98 ± 0.05	3.35 ± 0.32	
	1-butene	1.14 ± 0.03	3.86 ± 0.56	
		1.12 ± 0.03	3.78 ± 0.55	
		1.15 ± 0.04	3.90 ± 0.57	

Reaction	Reference	$(k_{SA}/k_R) \pm 2\sigma$	$(k_{SA} \pm 2\sigma)^a/10^{-12}$	$(\overline{k}_{SA} \pm 2\sigma)^b/10^{-12}$
3,3DM1BuOH + OH	Isopropanol	1.00 ± 0.04	5.09 ± 0.20	5.33 ± 0.16
		1.13 ± 0.09	5.78 ± 0.47	
		1.12 ± 0.08	5.72 ± 0.40	
	2-methyl-2-butanol	1.60 ± 0.09	5.78 ± 1.01	
		1.57 ± 0.08	5.65 ± 1.00	
		1.61 ± 0.09	5.79 ± 1.02	
3,3DM2BuOH + OH	Isopropanol	2.33 ± 0.09	11.90 ± 0.48	10.50 ± 0.25
		2.05 ± 0.08	10.50 ± 0.45	
		1.95 ± 0.08	9.95 ± 0.43	
	2-methyl-2-butanol	2.39 ± 0.09	8.61 ± 1.50	
		2.92 ± 0.09	10.50 ±1.78	
		2.25 ± 0.09	8.12 ± 1.34	
4MCHexOH + OH	Propene	0.64 ± 0.01	17.10 ± 2.59	18.70 ± 1.42
		0.76 ± 0.03	20.30 ± 3.19	
		0.76 ± 0.02	20.40 ± 3.10	
	Cyclohexene	0.27 ± 0.01	18.20 ± 4.55	
		0.27 ± 0.01	18.40 ± 4.62	
		0.27 ± 0.01	18.00 ± 4.46	

Reaction	Reference	$(k_{SA}/k_R) \pm 2\sigma$	$(k_{SA} \pm 2\sigma)^a/10^{-15}$	$(\overline{k}_{SA} \pm 2\sigma)^b/10^{-15}$
4MCHexOH + NO_3	1-butanol	1.08 ± 0.12	3.39 ± 1.11	2.69 ± 0.37
		1.81 ± 0.15	5.70 ± 1.82	
		0.79 ± 0.07	2.51 ± 0.80	
	2-ethyl-1-hexanol	0.71 ± 0.10	2.08 ± 0.72	
		1.00 ± 0.10	2.93 ± 0.96	
		0.86 ± 0.08	2.52 ± 0.82	

[a]The uncertainties for rate coefficients of SAs (σ_{SA}) were calculated from the uncertainty of slope of plots (σ_{slope}) and the uncertainty of the reference (σ_{kR}) by using the propagation of uncertainties. [b]Weighted average according to the equation $(w_1k_1 + w_2k_{2+}...)/(w_1 + w_2...)$; $(w_i = 1/\sigma_i^2)$. The uncertainty of weighted average (σ) was given by $(1/w_1 + 1/w_2 + ...)^{-0.5}$.

Table 2. Estimated and experimental rate coefficients (k_{SAR}, k_{log} and k_{exp}) for the reaction of SAs with atmospheric oxidants and ratio of rate coefficients (k_{exp}/k_{SAR} and k_{exp}/k_{log}). $k_{Cl}/10^{-11}$, $k_{OH}/10^{-12}$ and $k_{NO3}/10^{-15}$ in cm^3 molecule^{-1} s^{-1} units.

	4MCHexOH			3,3DM1ButOH			3,3DM2ButOH		
	k_{Cl}	k_{OH}	k_{NO3}	k_{Cl}	k_{OH}	k_{NO3}	k_{Cl}	k_{OH}	k_{NO3}
k_{exp}	37.0[a]	18.7[a]	2.69[a]	26.9[a]	5.33[a]	1.78[b]	12.1[a]	10.5[a]	3.4[b]
k_{SAR}	34.2[c]	19.2[c]	2.27[c]	21.0[c]	6.08[c]	0.55[c]	15.2[c]	9.16[c]	3.86[c]
k_{exp}/k_{SAR}	1.08	0.97	1.18	1.28	0.88	3.24	0.80	1.15	0.88
k_{log}	30.7[d]	-	4.69[d]	13.9[d]	-	1.16[d]	21.4[d]	-	3.19[d]
k_{exp}/k_{log}	1.21	-	0.57	1.94	-	1.53	0.57	-	1.07

[a] Data obtained in this work.
[b] Data obtained by Moreno et al., 2014.
[c] See S2 Supplementary Material.
[d] Estimated using the correlations log$_{Cl}$-log$_{OH}$ (Eq. (2)) and log$_{NO3}$-log$_{OH}$ (Eq. (3)) described by Calvert et al, 2011.

1 **Table 3.** Experimental conditions and molecular yields of E-4-methylcyclohexanone for the reaction
2 of 4MCHexOH with atmospheric oxidants.

SA	Oxidant	Exp	[SA] (ppm)	[Precursor] (ppm)	[NO] (ppm)	Carbonyl compound [d]Yield (%)	Technique	Average[f] (%)	SAR Yield (%)
	Cl[a]	1	3	21	-	24.8±0.9	FTIR	25.2±1.9	
		2	8	22	-	23.8±0.6	FTIR		
		3	13	16	-	27.5±0.2	SPME/GC-TOFMS[e]		14
	Cl[a] + NO	1	11	23	30	30.4±0.9	FTIR	29.5±0.7	
		2	5	25	19	30.0±0.6	FTIR		
		3	7	13	12	31.6±1.3	SPME/GC-TOFMS[e]		
4MCHexOH	OH[b]	1	7	36	23	35.1±1.3	FTIR		
		2	13	31	29	38.2±1.5	FTIR		
		3	11	28	28.5	47.8±0.4	FTIR	40.2±5.4	53
		4	6	19	12	39.8±0.9	SPME/GC-TOFMS[e]		
	NO₃[c]	1	3	6	-	56.8±11.4	SPME/GC-TOFMS[e]		
		2	6	34	-	88.3±7.0	SPME/GC-TOFMS[e]	58.0±23.5	86
		3	4	30	-	77.1±4.6	SPME/GC-TOFMS[e]		
		4	4	21	-	34.6±0.5	FTIR		
		5	7	10	-	33.4±0.6	FTIR		

3 [a]Rate coefficient, k (in cm^3 molecule^{-1} s^{-1} unit) used to correct the concentration of E-4-methylcyclohexanone by
4 loss with the reaction of Cl atoms = 11.2×10^{-11} (data of 2-methylcyclohexanone and Cl atoms (Herath et al.,
5 2018)). Photolysis rate coefficient estimated for E-4-methylcyclohexanone under our experimental conditions, k_p
6 =5×10^{-5} s^{-1}.

7 [b]Rate coefficient, k (in cm^3 molecule^{-1} s^{-1} unit) used to correct the concentration of E-4-methylcyclohexanone by
8 loss with the reaction of OH radical =13.7×10^{-12} (estimated using AOPWIN, v1.92). Photolysis rate coefficient
9 estimated for E-4-methylcyclohexanone under our experimental conditions, k_p =5×10^{-5} s^{-1}.

10 [c]Rate coefficient k (in cm^3 molecule^{-1} s^{-1} unit) used to correct the concentration of E-4-methylcyclohexanone by
11 loss with the reaction of NO₃ radical = 2.28×10^{-16} (estimated using SAR method, Kerdouci et al., 2014).

12 [d]Indicated errors are the associated errors, to the slope of plots obtained in the least squares analysis.

13 [e]Experiment using a Teflon gas bag of 150L.

14 [f] Standard deviations 1σ.

15

| 1 | **Table 4.** Experimental conditions and molecular yields of 3,3-dimethylbutanal for the reaction of |
| 2 | 3,3DM1ButOH with atmospheric oxidants. |

SA	Oxidant	Exp	[SA] (ppm)	[Precursor] (ppm)	[NO] (ppm)	Carbonyl compound [f]Yield (%)	Technique	Average[g] (%)	SAR Yield (%)
	Cl[a]	1	11	24	-	40.3±0.2	FTIR		
						41.8±4.6	SPME/GC-TOFMS[d]	39.4±15.0	
		2	2.6	8	-	19.6±0.5	SPME/GC-TOFMS[e]		
		3	6	25	-	55.9±1.7	FTIR		
	Cl[a] + NO	1	10	21	21	61.6±3.4	FTIR		40
						34.7±4.4	SPME/GC-TOFMS[d]	43.3±17.7	
3,3DM1ButOH		2	4	9	8	23.0±4.2	SPME/GC-TOFMS[e]		
		3	10	25	25	48.8±0.6	FTIR		
	OH[b]	1	10	60	36	82.1±4.2	FTIR		66
						40.8±2.7	SPME/GC-TOFMS[d]	62.2±15.0	
		2	7	35	57	67.4±1.4	FTIR		
		3	11	28	55	61.9±0.9	FTIR		
		4	11	29	30	59.1±3.8	FTIR		
	NO$_3$[c]	1	11	36	-	29.2±0.5	FTIR		86
						53.9 [h]	SPME/GC-TOFMS[d]	36.2±14.6	
		2	11	32	-	26.5±1.6	FTIR		

3 [a]Rate coefficient, k (in cm^3 molecule^{-1} s^{-1} unit) used to correct the concentration of 3,3-dimethylbutanal by loss

4 with the reaction of Cl atoms = 1.7 × 10^{-10} (data of iso-Butyraldehyde and Cl atoms (Thevenet et al., 2000)).

5 Photolysis rate coefficient estimated for 3,3-dimethylbutanal under our experimental conditions, k$_p$ = 1 × 10^{-4} s^{-1}.

6 [b]Rate coefficient, k (in cm^3 molecule^{-1} s^{-1} unit) used to correct the concentration of 3,3-dimethylbutanal by loss

7 with the reaction of OH radical = 2.73 × 10^{-11} (Aschmann et al., 2010). Photolysis rate coefficient estimated for

8 3,3-dimethylbutanal under our experimental conditions, k$_p$ = 1 × 10^{-4} s^{-1}.

9 [c]Rate coefficient k (in cm^3 molecule^{-1} s^{-1} unit) used to correct the concentration of 3,3-dimethylbutanal by loss

10 with the reaction of NO$_3$ radical = 1.27 × 10^{-14} (D'Anna, 2001).

11 [d]Experiment using a FTIR gas cell of 50 L.

12 [e]Experiment using a Teflon gas bag of 150 L.

13 [f]Indicated errors are the associated errors to the slope of plots obtained in the least squares analysis.

14 [g]Standard deviations 1σ.

15 [h]Yield estimated using only one data.

16

1   **Table 5.** Experimental conditions and molecular yields of 3,3-dimethyl-2-butanone for the reaction
2   of 3,3DM2ButOH with atmospheric oxidants

SA	Oxidant	Exp	[SA] (ppm)	[Precursor] (ppm)	[NO] (ppm)	Carbonyl compound [f]Yield (%)	Technique	Average[g] (%)	SAR Yield (%)
	Cl[a]	1	14	31	-	42.8±0.7	FTIR		
						45.2±1.1	SPME/GC-TOFMS[d]		
		2	2.3	8	-	41.7±3.2	SPME/GC-TOFMS[e]	43.2±1.8	
	Cl[a] + NO	1	14	28	20	36.7±5.0	FTIR		40
						49.6±4.5	SPME/GC-TOFMS[d]	44.2±7.4	
3,3DM2ButOH		2	3	7	6	39.0±6.1	SPME/GC-TOFMS[e]		
		3	8	28	27	51.5±3.9	FTIR		
	OH[b]	1	8	55	42	82.8±3.1	FTIR		
						71.2±2.6	SPME/GC-TOFMS[d]	80.7±6.5	91
		2	5	66	36	85.4±5.8	FTIR		
		3	11	28	29	83.6±3.0	FTIR		
	NO$_3$[c]	1	12	30	-	66.7±2.05	FTIR		
						45.9±1.6	SPME/GC-TOFMS[d]	58.0±10.9	99
		2	9	30	-	61.5±1.4	FTIR		

3   [a]Rate coefficient, k (in cm^3 molecule^{-1} s^{-1} unit) used to correct the concentration of 3,3-dimethyl-2-butanone by
4   loss with the reaction of Cl atoms = 4.8×10^{-11} (Farrugia et al., 2015)). Photolysis rate coefficient estimated for
5   3,3-dimethyl-2-butanone under our experimental conditions, $k_p = 7 \times 10^{-5}$ s^{-1}.

6   [b]Rate coefficient, k (in cm^3 molecule^{-1} s^{-1} unit) used to correct the concentration of 3,3-dimethyl-2-butanone by
7   loss with the reaction of OH radical = 1.21×10^{-12} (Wallington and Kurylo., 1987). Photolysis rate coefficient
8   estimated for 3,3-dimethyl-2-butanone under our experimental conditions, $k_p = 7 \times 10^{-5}$ s^{-1}.

9   [c]No corrected.

10   [d]Experiment using a FTIR gas cell of 50 L.

11   [e]Experiment using a Teflon gas bag of 150 L.

12   [f]Indicated errors are the associated errors to the slope of plots obtained in the least squares analysis.

13   [g]Standard deviations 1σ.

14

15

Table 6: Summary of molecular yields (%) of reaction products identified in the reaction of SAs with atmospheric oxidants and the total carbon balance (%).

Product	SA			
	4MCHexOH			
	Cl	**Cl + NO**	**OH**	**NO$_3$**
E-4-methylcyclohexanone[1]	25.2 ± 1.9	29.5 ± 0.7	40.2 ± 5.4	58.0 ± 23.5
HCOH[2]	9	-	-	-
Nitrated compounds	-	20	10	60
Total Carbon[3]	26	50	50	~100
	3,3DM1ButOH			
	Cl	**Cl + NO**	**OH**	**NO$_3$**
3,3-dimethylbutanal[1]	39.4 ± 15.0	43.3 ± 17.7	62.2 ± 15.0	36.2 ± 14.6
HCOH[2]	10	22	-	-
2,2-dimethylpropanal[2]	22	8	23	-
Acetone[2]	5	17	-	-
Nitrated compounds	-	40[5]	35[6]	200[7]
Total Carbon[3,4]	61	62	81	36
	3,3DM2ButOH			
	Cl	**Cl + NO**	**OH**	**NO$_3$**
3,3-dimethyl-2-butanone[1]	43.2 ± 1.8	44.2 ± 7.4	80.7 ± 6.5	58.0 ± 10.9
HCOH[2]	10	64	-	-
2,2-dimthylpropanal[2]	14	10	14	-
Acetone[2]	3	58	-	-
Acetaldehyde[2]	-	17	-	-
Nitrated compounds	-	30	20	120
Total Carbon[3,4]	~60	98	93	58

[1]Average Tables 3-5.

[2]Molecular yield obtained in earlier step of the reaction.

[3]$Total\ Carbon\ (\%) = \sum_{1}^{i}\left(\frac{n^{\circ}\ of\ carbon\ of\ product_i}{n^{\circ}\ of\ carbon\ of\ SA} \times molar\ yield_i(\%)\right)$

[4]Nitrate compounds were not accounted for.

[5]From analysis of the experiment number 3 for the reaction of Cl in the presence of NO$_x$.

[6]From average of experiments number 2, 3 and 4 for the reaction with OH.

[7]From analysis of the experiments number 1 and 2 for reaction with NO$_3$.

Table 7. Lifetimes of 4MCHexOH, 3,3DM1ButOH and 3,3DM2ButOH.

	τ_{OH} (days)	τ_{Cl} [a](days)	τ_{Cl} [b](days)	τ_{NO3} (days)	τ_{wet} (years)	τ_{global}[a](days)
4MCHexOH	0.62	31.28	0.24	8.61	~2.1	0.58
3,3DM1ButOH	2.17	43.03	0.33	13[c]	~15.8	1.78
3,3DM2ButOH	1.10	95.65	0.74	6.73[c]	11.3	0.94

12   [a]Determined with the 24 hours average of chlorine atoms.

13   [b]Determined with the peak concentration of chlorine atoms.

14   [c]Determined using the rate coefficient obtained by Moreno et al., 2014.

15

1   A)
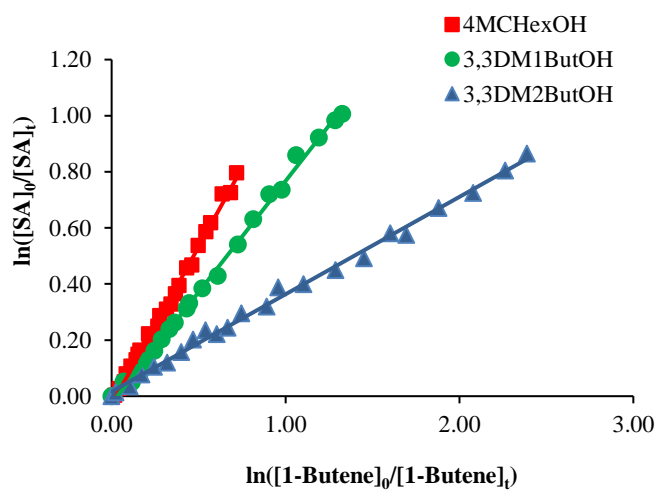
2
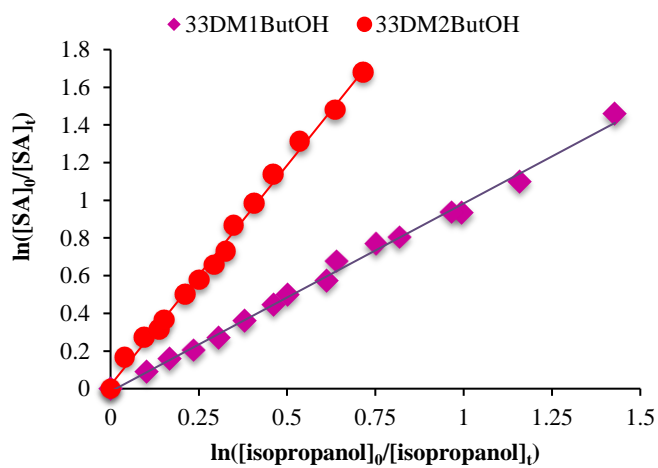
3   B)

4   C)
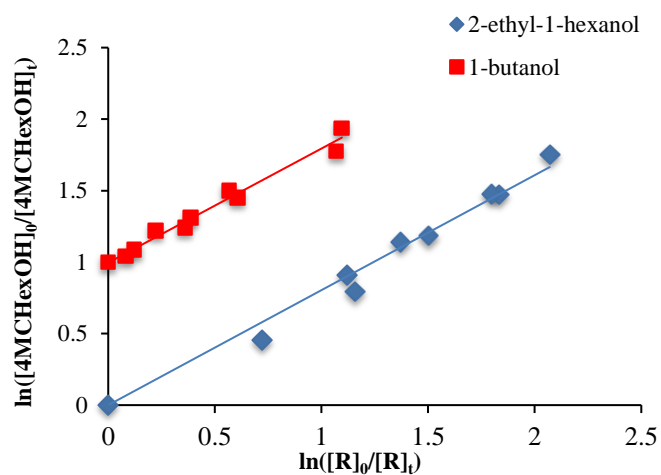
5

6   Fig.1: Relative rate plots for the reaction of (A) SAs with chlorine atoms employing 1-butene as a reference
7   compound (B) 3,3-dimethylbutanols and OH radical with isopropanol as a reference compound and (C)
8   4MCHexOH and NO_3 with two reference compounds. Data for 1-butanol have been vertically displaced for clarity.

1

2
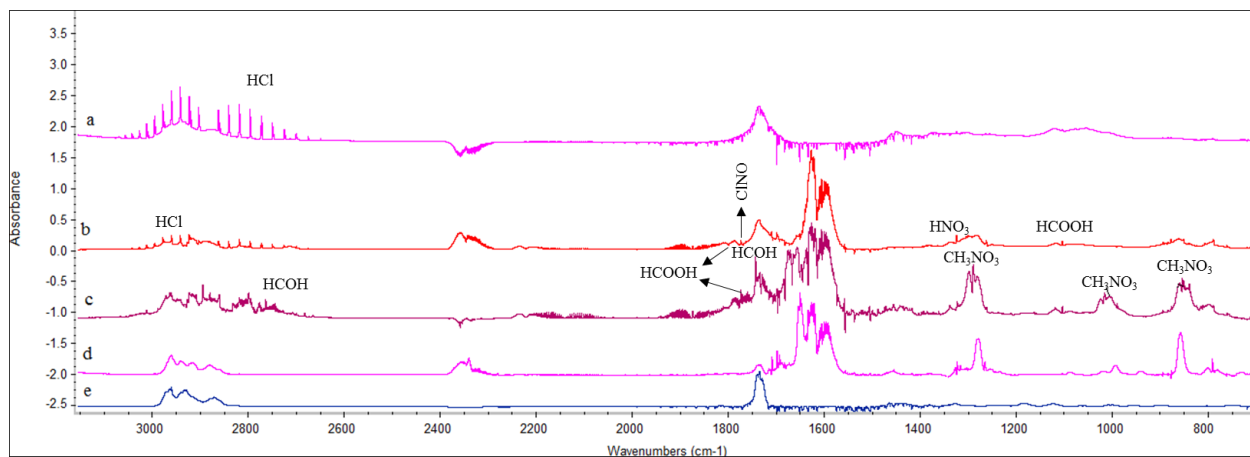
3
4
5 Fig. 2: Product spectra for reaction of 4MCHexOH with: (a) chlorine atoms at 10 min (x 2 to clarity), (b) Cl atoms
6 in presence of NOx at 7 min. (c) OH radical at 40 min and (d) NO$_3$ radical at 32 min. (e) Spectrum of 4-
7 methylcyclohexanone commercial sample.
8
9
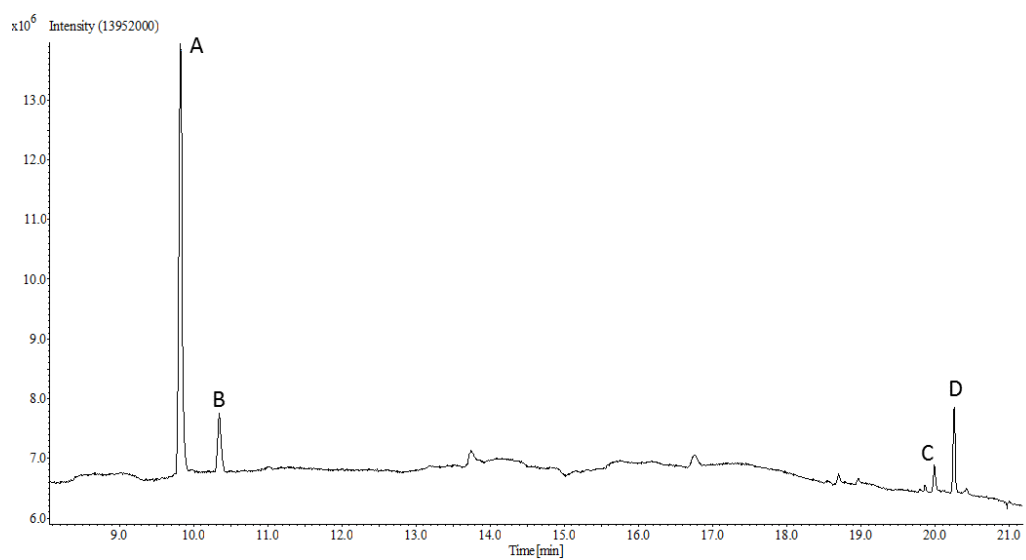
Fig. 3: SPME/GC-TOFMS chromatogram for the reaction of 4MCHexOH with Cl atoms after 15 minutes of reaction. Peak (A) 4MCHexOH. Peak (B) E-4-methylcyclohexanone. Peaks (C) and (D) reaction products.
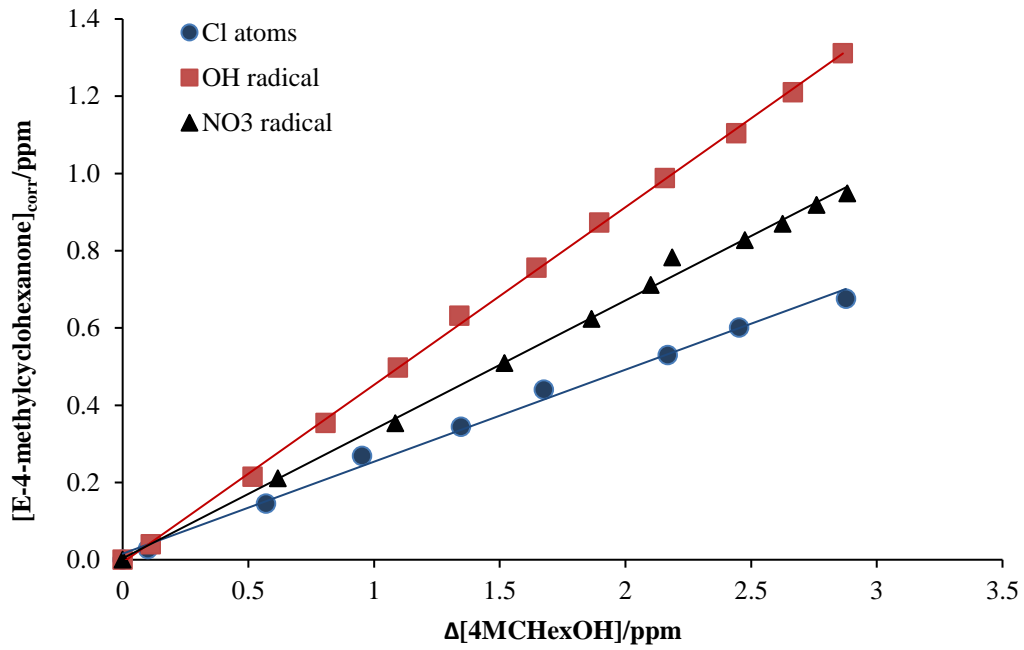
Fig. 4: Plots of corrected concentration of E-4-methylcyclohexanone ([E-4-methylcyclohexanone]$_{corr}$) against 4MCHexOH consumed (Δ[4MCHexOH]) for Cl atoms (in the absence of NOx) and OH and NO$_3$ radical reactions.
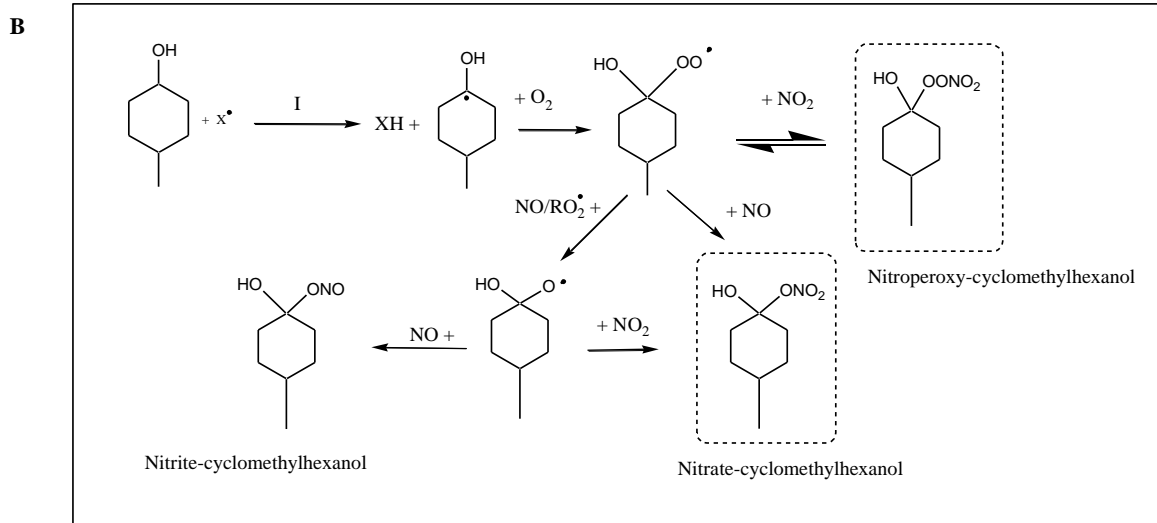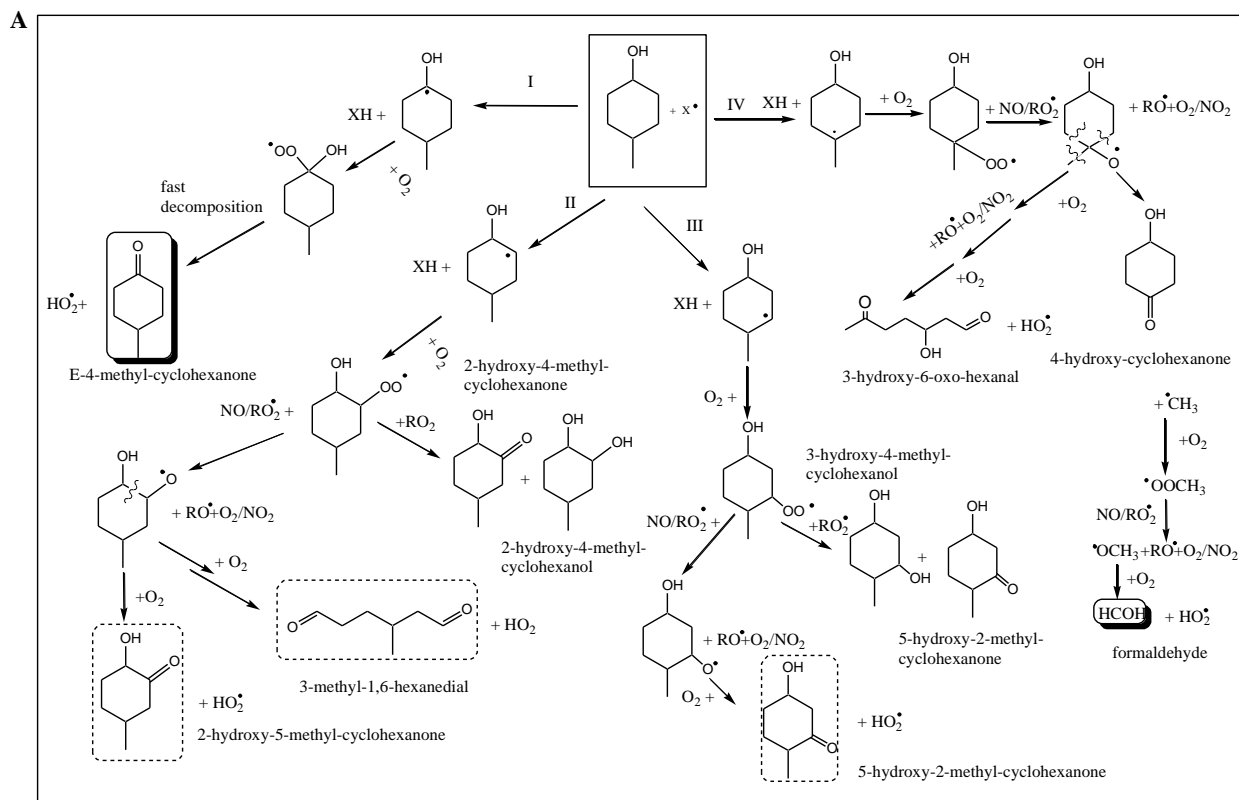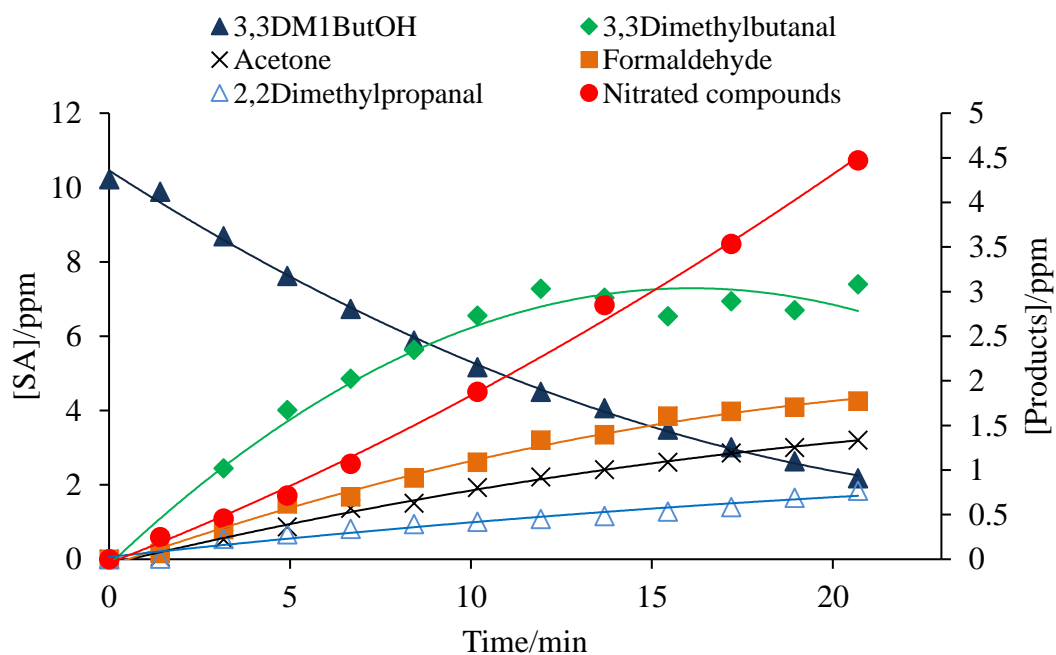
Fig. 5: Reaction mechanism for the degradation of 4MCHexOH with X (Cl atom, OH and NO$_3$ radicals). (A) Mechanism for the formation of carbonyl compounds. (B) Mechanism for the formation of nitrated compounds. Compounds marked with solid line are positively identified. Compounds marked with dotted lines are not positively identified.
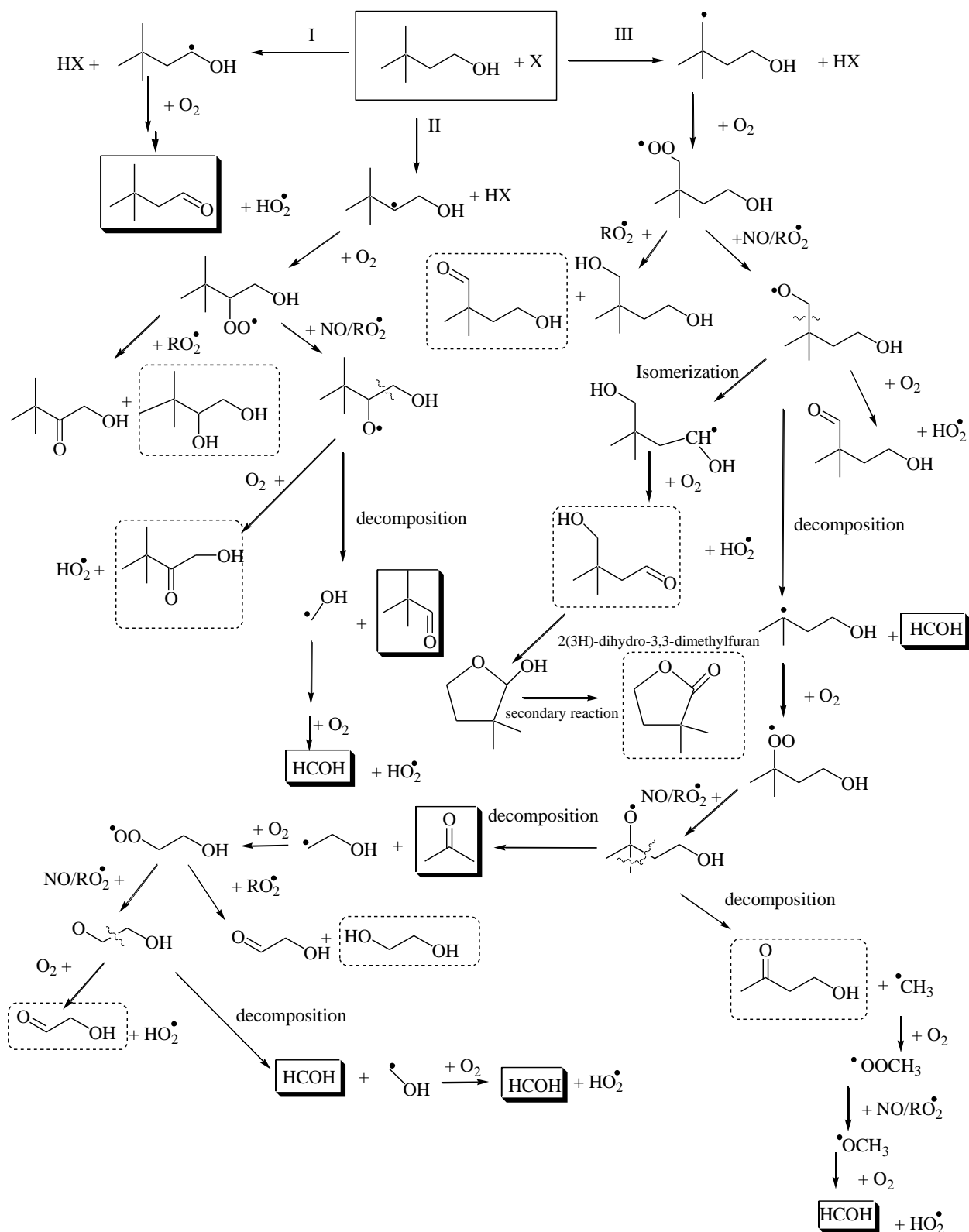
1   A)
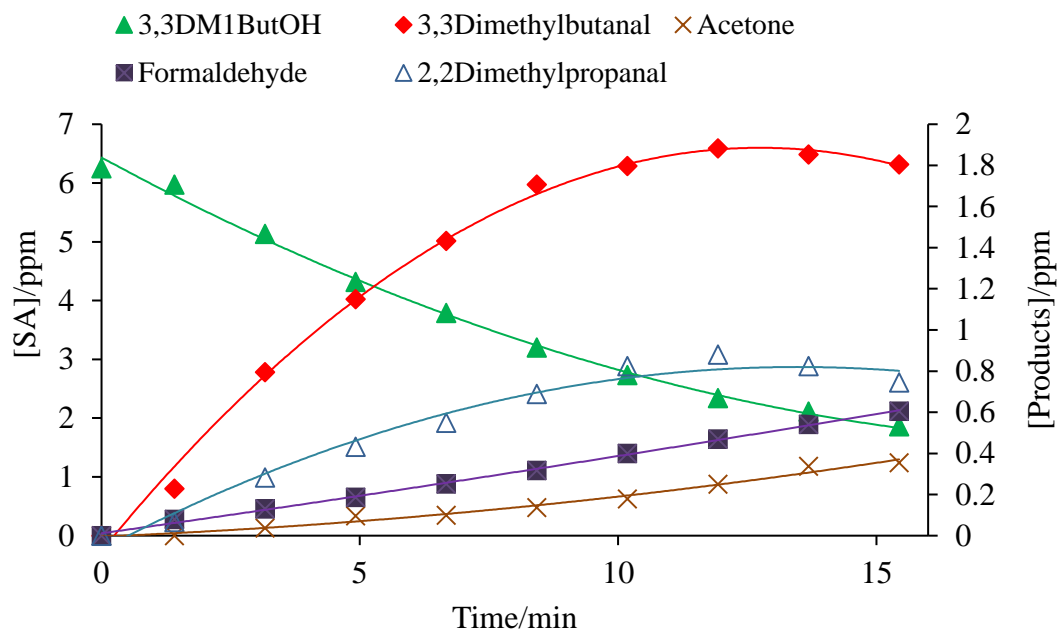
2

3   B)

4

5   Fig. 6: Concentration-time profiles of SA (3,3DM1ButOH) and reaction products formed in the reaction of
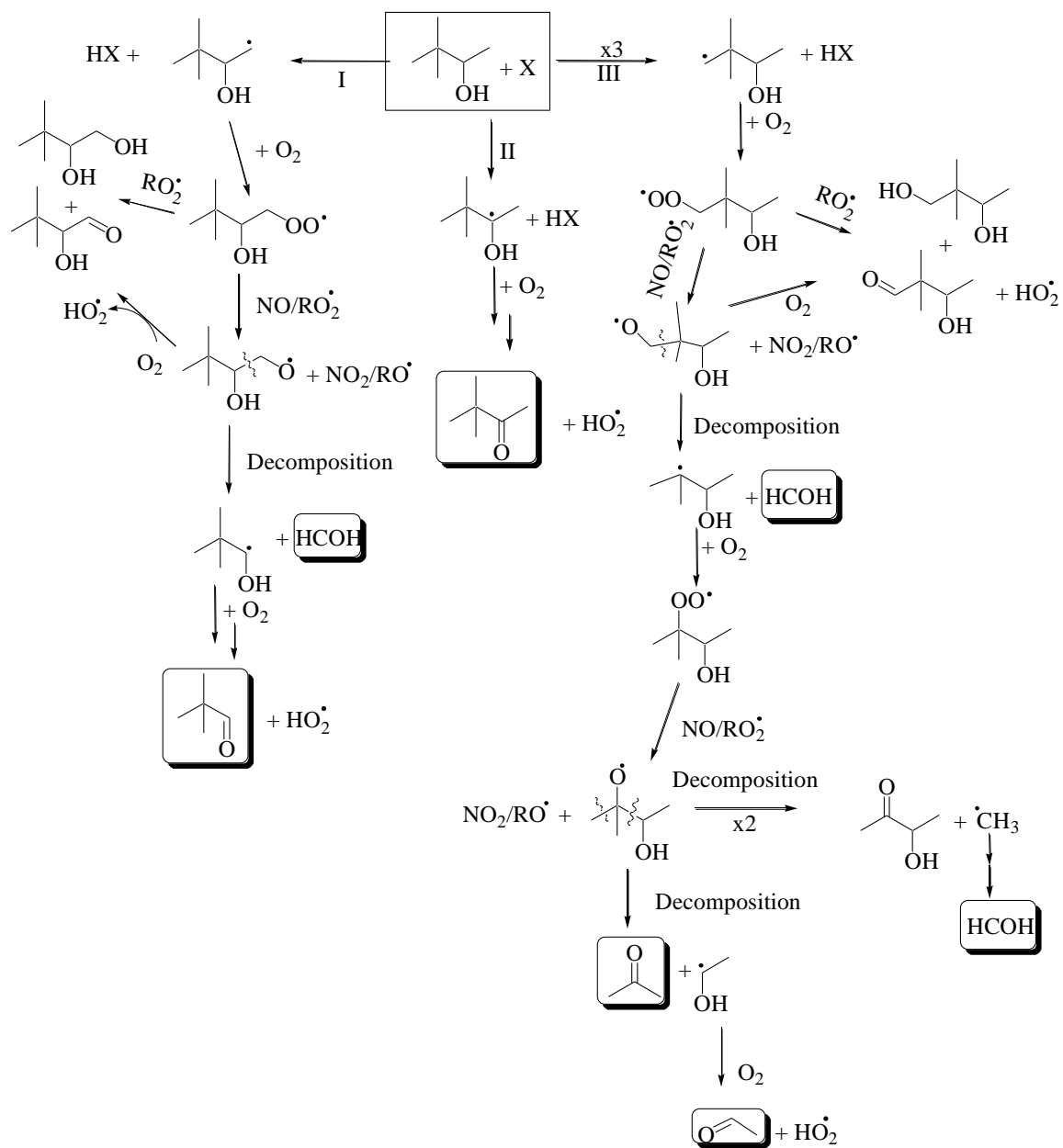6   3,3DM1ButOH with Cl atoms in the absence (A) and in the presence of NO_x (B).

7

1
2

Fig. 7: Reaction mechanism for the degradation of 3,3DM1ButOH with X (Cl atom, OH and NO$_3$ radical).
Mechanism for the formation of carbonyl compounds. Compounds marked with solid line are positively identified.
Compounds marked with dotted lines are not positively identified.

6
7

Fig. 8: Reaction mechanism for the degradation of 3,3DM2ButOH with X (Cl atom, OH and NO₃ radical). Mechanism to form carbonyl compounds. Compounds marked with solid line are positively identified. Compounds marked with dotted lines are not positively identified.